SANT proteins modulate gene expression by coordinating histone H3KAc and Khib levels and regulate plant heat tolerance

SANT proteins modulate gene expression by coordinating histone H3KAc and Khib levels and regulate plant heat tolerance

Xishi Zhou[1], Yujin Fan[1,2,3], Xiying Zhu[1,2,3], Ruihua Zhao[1], Junna He[4], Pengfeng Li[1], Shengping Shang[1], Justin Goodrich[5], Jian-Kang Zhu[6,7], Cui-Jun Zhang[1*]

[1] Shenzhen Branch, Guangdong Laboratory of Lingnan Modern Agriculture, Key Laboratory of Synthetic Biology, Ministry of Agriculture and Rural Affairs, Agricultural Genomics Institute at Shenzhen, Chinese Academy of Agricultural Sciences, Shenzhen 518120, China;

[2] School of Life Sciences, Henan University, Kaifeng 475004, China

[3] Shenzhen Research Institute of Henan University, Shenzhen 518000, China

[4] College of Horticulture, China Agricultural University, Beijing, 100193 China

[5] Institute of Molecular Plant Science, School of Biological Sciences, University of Edinburgh, Daniel Rutherford Building, Max Born Crescent, Edinburgh, EH9 3BF, United Kingdom

[6] Institute of Advanced Biotechnology and School of Life Sciences, Southern University of Science and Technology, Shenzhen, China

[7] Center for Advanced Bioindustry Technologies, Chinese Academy of Agricultural Sciences, Beijing, China

* Correspondence: Cui-Jun Zhang (zhangcuijun@caas.cn)

Short title: SANT proteins regulate plant heat tolerance

One-sentence summary: Proteins containing a histone-tail-binding module coordinate histone lysine acetylation and 2-hydroxyisobutyrylation and play critical roles in transcriptional regulation and plant thermotolerance.

The author responsible for distribution of materials integral to the findings presented in this article in accordance with the policy described in the Instructions for Authors (https://academic.oup.com/plphys/pages/General-Instructions) is Cui-Jun Zhang.

Abstract

Histone post-translational modifications (PTMs), such as acetylation and recently identified lysine 2-hydroxyisobutyrylation (Khib), act as active epigenomic marks in plants. SANT domain-containing proteins SANT1, SANT2, SANT3 and SANT4 (SANT1/2/3/4), derived from *PIF/Harbinger* transposases, form a complex with HISTONE DEACETYLASE 6 (HDA6) to regulate gene expression via histone deacetylation. However, whether SANT1/2/3/4 coordinate different types of PTMs to regulate transcription and mediate responses to specific stresses in plants remains unclear. Here, in addition to modulating histone deacetylation, we found that SANT1/2/3/4 proteins acted like HDA6 or HDA9 in regulating the removal of histone Khib in Arabidopsis (*Arabidopsis thaliana*). Histone H3 lysine acetylation (H3KAc) and histone Khib were coordinated by SANT1/2/3/4 to regulate gene expression, with H3KAc playing a predominant role and Khib acting complementarily to H3KAc. *SANT1/2/3/4* mutation significantly increased the expression of heat-inducible genes with concurrent change of H3KAc levels under normal and heat stress conditions, resulting in enhanced thermotolerance. This study revealed the critical roles of *Harbinger* transposon-derived SANT domain-containing proteins in transcriptional regulation by coordinating different types of histone PTMs and in the regulation of plant thermotolerance by mediating histone acetylation modification.

Introduction

In eukaryotic cells, chromatin is decorated by various epigenetic marks, such as DNA methylation and histone post-translational modifications (PTMs). Histone PTMs, such as acetylation, methylation, ubiquitination, and phosphorylation, affect the chromatin state and gene expression (Garcia et al., 2007; Zhao et al., 2019). Histone lysine acetylation (KAc), a prominent modification, is associated with transcriptional activation (Shahbazian and Grunstein, 2007). Various short-chain fatty acid acylation modifications on lysine residues, including 2-hydroxyisobutyrylation (Khib), crotonylation (Kcr), butyrylation (Kbu), and

hydroxybutyrylation, have been identified (Chen et al., 2007; Dai et al., 2014; Kebede et al., 2017). In Arabidopsis (*Arabidopsis thaliana*), histone Khib is highly enriched at the transcription start site (TSS) to promote gene expression (Zheng et al., 2021). Khib is a conserved active epigenomic mark in plants involved in several biological processes, including protein synthesis and degradation, glycolysis/gluconeogenesis, and the tricarboxylic acid cycle (Yu et al., 2017; Zhang et al., 2022). The mechanism by which histone Khib functionally interacts with KAc has attracted widespread attention. H4K8hib acts synergistically with KAc to orchestrate diverse cellular processes by regulating gene expression in yeast and mammals (Huang et al., 2017; Huang et al., 2018). In Arabidopsis, Khib functions in concert with H3K23Ac to maintain high transcriptional outputs and regulate cellular metabolism (Zheng et al., 2021). These results warrant further investigation of the mechanism determining and coordinating the presence of the two modifications to regulate gene transcription in plants.

Level of histone acetylation is determined by the activity of histone acetyltransferases (HATs) and deacetylases (HDAs or HDACs). HDAs such as HDA6 and HDA9 remove acetylation marks from histone lysine sites and mediate transcriptional repression in Arabidopsis (Allfrey et al., 1964; Yruela et al., 2021). In addition, HDA6 and HDA9 are major candidates of histone Khib erasers in Arabidopsis (Zheng et al., 2021). Histone modifications mediated by HDA6 and HDA9 are involved in various biological processes, such as transcriptional silencing, flowering regulation, and stress responses in plants. For example, HDA9 negatively regulates plant immunity and HDA6 represses pathogen defense responses in Arabidopsis (Wang et al., 2017; Yang et al., 2020). Furthermore, Histone H3K23ac and Khib are co-enriched on genes involved in cellular metabolism to fine-tune the plant responses to dark-induced starvation (Zheng et al., 2021).

High temperature stress due to global warming seriously affect plant growth and development and substantially reduce crop yields. Plants have evolved various regulatory mechanisms to respond to high temperature and to alleviate heat stress damage. Central to the heat stress (HS)

response in plants are the HS transcription factors, which are rapidly activated and bind to the promoters of heat shock protein (HSP) genes to induce *HSP* expression when plants are subjected to HS (Bourgine and Guihur, 2021). Epigenetic modifications also play critical roles in preventing heat damage and enhancing plant thermotolerance (He & Li, 2018; Perrella et al., 2022). The histone acetyltransferase, GCN5, enhances heat responsive gene expression and plant thermotolerance by increasing H3K9Ac and H3K14Ac levels in the promoter region of *ULTRAVIOLET HYPERSENSITIVE 6* (*UVH6*) in Arabidopsis (Hu et al., 2015; Hu et al., 2019). A conserved HS response mechanism involves HDA9 translocation from the cytoplasm to the nucleus to bind to and deacetylate target genes related to signal transduction and plant development, resulting in a trade-off between plant development and the HS response (Niu et al., 2022). Plant-specific histone deacetylase HD2B- and HD2C-regulated histone acetylation and DNA methylation play key roles in heterochromatin stabilization under HS (Yang et al., 2023).

Transposable elements and repetitive sequences, which constitute a large proportion of the eukaryotic genome, are important contributors to the emergence of novel host genes via molecular domestication. *PIF*/*Harbinger* class transposons are a DNA transposon superfamily that encode two proteins: nuclease and SANT/myb/trihelix domain-containing DNA-binding protein (Kapitonov and Jurka, 2004; Zhang et al., 2004). The two components of *Harbinger* transposases are typically co-domesticated as an interacting pair, as with ANTAGONIST OF LIKE HETEROCHROMATIN PROTEIN 1 (ALP1)/ALP2, HARBINGER-DERIVED PROTEIN 1 (HDP1)/HDP2, and HARBINGER FAMILY OF PLANT TRANSPOSASE 1 (HHP1)/SANT domain-containing proteins (SANT1/2/3/4) in Arabidopsis. Interestingly, these three pairs have been proposed to be components of different chromatin-modifying complexes that play key roles in regulating gene expression (Liang et al., 2015; Duan et al., 2017; Velanis et al., 2020; Feng et al., 2021; Zhou et al., 2021). The four SANT domain-containing proteins (functionally redundant) domesticated from *PIF*/*Harbinger* transposases and identified in our previous study can form a histone deacetylase complex with HDA6 to regulate the expression

of common target genes via histone deacetylation as well as the flowering time (Feng et al., 2021; Zhou et al., 2021). Gene Ontology (GO) term enrichment analysis revealed that genes differentially expressed in the higher-order *SANT1/2/3/4* mutants are significantly enriched in biotic and abiotic stress responses (Feng et al., 2021; Zhou et al., 2021). However, the specific roles of SANT1/2/3/4 in plant stress responses remain unclear.

In this study, we demonstrated that SANT1/2/3/4 proteins co-regulate histone Khib with HDA6 or HDA9 in the genome and *sant-null*-mediated transcriptional activation was associated with higher histone Khib levels. Histone Khib is highly correlated with acetylation in Arabidopsis. Interestingly, SANT1/2/3/4 regulate H3KAc and histone Khib mostly at different sites. As active epigenomic marks, the increased H3KAc and histone Khib levels act in combination, not antagonistically, to maintain high transcriptional outputs in *sant-null* mutant, with H3KAc playing a predominate role. In addition, a small proportion of upregulated genes in *sant-null* had lower levels of H3KAc and higher levels of histone Khib compared to Col-0, suggesting that histone Khib may substitute for H3KAc to promote gene expression. *SANT1/2/3/4* mutation significantly increased the expression levels of heat-inducible (HI) genes with concurrent change of H3KAc levels under normal and HS conditions, resulting in enhanced thermotolerance. Taken together, our findings highlight the critical roles of *Harbinger* transposon-derived SANT domain-containing proteins in transcriptional regulation by coordinating histone PTMs and in plant thermotolerance by regulating H3KAc levels.

Results

SANT1/2/3/4 co-regulate histone Khib with HDA6 or HDA9 to repress gene expression

HDA6 and HDA9 are involved in removing histone Khib (Zheng et al., 2021). Interaction between SANT1/2/3/4 and HDA6 prompted us to examine the role of SANT1/2/3/4 proteins in histone Khib regulation. Compared to Col-0, histone Khib ChIP-seq revealed 2429, 2114, and 2188 regions with significantly higher levels of histone Khib in *sant-null*, *hda6*, and *hda9* mutants, respectively (Supplementary Table S1). Metaplot and heatmap analysis revealed that

the histone Khib levels of *sant-null* up-Khib peaks were substantially increased in both *hda6* and *hda9* mutants compared to those in Col-0 (Figure 1A). Histone Khib levels of *hda6* or *hda9* up-Khib peaks were also obviously increased in *sant-null* mutant (Supplementary Figure S1A and Supplementary Figure S2A). Genome annotation of *sant-null*, *hda6*, and *hda9* up-Khib peaks demonstrated that genes with increased histone Khib in *sant-null* mutant largely overlapped with those in *hda6* or *hda9* mutants (Figure 1B and Supplementary Table S2), suggesting that SANT1/2/3/4 co-regulate histone Khib with HDA6 or HDA9. Two hundred and ninety-one genes with increased histone Khib levels in *sant-null*, *hda6* and *hda9* mutants were mainly involved in transcriptional regulation, mRNA metabolism, nuclear transport and plant compound catabolic and metabolic processes (Figure 1B and Supplementary Figure S3).

As histone Khib is abundant in genic regions and positively related to gene expression, we further investigated the contribution of SANT1/2/3/4 mediated histone Khib in transcriptional regulation. Although only 103 out of the 2371 *sant-null* mediated up-Khib genes were significantly upregulated in *sant-null* compared to Col-0, the extent of this overlap was statistically significant, whereas only 30 out of the *sant-null* mediated up-Khib genes were significantly downregulated (Figure 1C). The relative histone Khib levels (*sant-null*/Col-0) were obviously higher in those 103 genes than the remaining 2268 *sant-null* up-Khib genes (Figure 1D), implying that *sant-null*-mediated transcriptional activation was associated with higher histone Khib levels. To confirm the function of SANT1/2/3/4 proteins at these 103 genes, we analyzed the enrichment of SANT3 using published ChIP-seq data (Wang et al., 2024). SANT3 displayed strong enrichment at these 103 gene regions, indicating that SANT proteins can localize to specific sites of the genome to regulate histone Khib modifications and gene expressions (Supplementary Figure S4A). Four representative loci visualized in IGV showed that SANT3-FLAG ChIP-seq signal, histone Khib levels and gene expression levels were obviously increased in *sant-null* mutant and RT-qPCR and ChIP-qPCR detection validated the increasement (Supplementary Figure S4B, S5). In addition, boxplot and metaplot analysis revealed that the average histone Khib levels of *sant-null* upregulated genes were

significantly increased in *sant-null*, *hda6* and *hda9* compared to Col-0 (Figure 1E and Supplementary Table S3). 607 out of 924 (66%) *hda6* upregulated genes showed obviously higher histone Khib levels in *hda6*, and most of those 607 genes also showed significantly higher histone Khib levels in *sant-null* compared to Col-0 (Supplementary Figure S1B, C and Supplementary Table S3). We analyzed previously reported RNA-seq data for *hda9* (Kim et al., 2016) and identified 738 upregulated and 573 downregulated genes in *hda9* compared to Col-0 (Supplementary Table S4). Similarly, 394 out of the 738 (53%) *hda9* upregulated genes showed obviously higher histone Khib levels in *hda9*, and most of those 394 genes also showed significantly higher histone Khib levels in *sant-null* compared to Col-0 (Supplementary Figure S2B, C and Supplementary Table S3). Taken together, the results above indicated that SANT1/2/3/4 co-regulated histone Khib with HDA6 or HDA9 to repress gene expression.

SANT1/2/3/4 regulate gene expression by coordinating H3KAc and histone Khib

It was reported that the H3K23Ac and histone Khib modifications act in combination to promote gene expression in Arabidopsis (Zheng et al., 2021). Thus, the observation that SANT1/2/3/4 proteins can regulate H3KAc and histone Khib prompted us to investigate the role of SANT1/2/3/4 in coordinating the presence of those two modifications to jointly determine gene expression level. We identified 11807 out of 21323 (55%) histone Khib peaks in Col-0 were also marked by H3KAc (Figure 2A). Interestingly, few *sant-null* up-H3KAc peaks were marked as *sant-null* up-Khib peaks, as evidenced by the weak overlap between *sant-null* mediated up-H3KAc and up-Khib genes (Figure 2B, C). Consistently, no obvious difference was found between Col-0 and *sant-null* in H3KAc levels of *sant-null* up-Khib peaks and vice versa (Figure 2D, E), suggesting that SANT1/2/3/4 regulated H3KAc and histone Khib mostly at different regions of genome.

To unveil the role of SANT1/2/3/4 mediated H3KAc and histone Khib in regulating gene expression via a synergistic or antagonistic manner, we analyzed H3KAc and histone Khib levels and expression levels of different group of genes in *sant-null*. The relative H3KAc and

histone Khib levels of *sant-null* upregulated genes were significantly higher than those of downregulated genes or of all genes (Figure 3A), indicating that H3KAc and histone Khib regulated by SANT1/2/3/4 act in concert, not antagonistically, to regulate gene expression. Genes gained H3KAc alone and genes gained both of the modifications in *sant-null* showed significantly higher relative expression (*sant-null*/Col-0) compared to the genome-wide, but genes gained histone Khib alone in *sant-null* showed no obvious expression changes (Figure 3B), indicating that H3KAc played a predominant role in SANT1/2/3/4-mediated transcriptional regulation. In our previous study, we found that H3KAc levels in a small portion of *sant-null* upregulated genes (138) did not increase compared to those in Col-0 (Zhou et al., 2021). However, SANT3-Flag displayed strong enrichment at these small portion of genes (Supplementary Figure S6). We thus determined the histone Khib levels of these 138 genes and found that histone Khib levels were higher in *sant-null* compared to Col-0 (Figure 3C, D), suggesting that increased histone Khib caused by *SANT1/2/3/4* mutation may act as a complementary epigenomic mark to H3KAc to activate gene expression. Two representative loci visualized in IGV and RT-qPCR and ChIP-qPCR validation showed that transcript and histone Khib levels were obviously increased in *sant-null*, but histone H3 acetylation levels were not increased (Figure 3E and Supplementary Figure S7). Collectively, our results indicated that although there was low concurrence of those two marks targeted by SANT1/2/3/4, H3KAc and histone Khib were coordinated by SANT1/2/3/4 to jointly regulate target gene expression.

SANT1/2/3/4 negatively regulate plant thermotolerance

GO enrichment analysis revealed that a significant fraction of the upregulated genes in *sant-null* participated in the stress responses (Feng et al., 2021; Zhou et al., 2021). Here, we found that the expression levels of the heat-responsive genes, *HEAT-INDUCED TAS1 TARGET 1* (*HTT1*) and *HTT4*, which are known to enhance plant thermotolerance, were remarkably increased in *sant-null* and to a lesser extent in *hda6* than in Col-0 (Supplementary Figure S8). Therefore, we examined the thermotolerance of Col-0, s*ant-null*, and *hda6* plants to

HS. Similar to Col-0, *sant-null* and *hda6* mutants grew normally under normal conditions (Figure 4A and Supplementary Figure S9A, B). Interestingly, *sant-null* exhibited enhanced thermotolerance, as evidenced by their higher survival rate after HS compared to Col-0 (Figure 4A, B). The thermotolerance and survival rates returned to Col-0 levels after HS treatment when the *sant-null* mutant was transformed with a genomic fragment encompassing *SANT3* (Figure 4C, D). Surprisingly, *hda6* exhibited impaired thermotolerance and a significantly lower survival rate than Col-0 under HS conditions (Figure 4A, B), which contradicted our previous observation that SANT1/2/3/4 can form a histone deacetylase complex with HDA6 to co-regulate the expression of common target genes. Therefore, SANT1/2/3/4 negatively regulate plant thermotolerance, probably in a HDA6-independent manner.

HI genes are significantly upregulated in *sant-null* mutant

To obtain insights into the role of SANT1/2/3/4 mediated transcriptional regulation in response to high temperature, we performed RNA-seq on seven-day-old Col-0 and *sant-null* seedlings grown under normal condition (22 °C) or exposed to 37 °C for 1 h. We also included *hda6* seedlings for comparison. The high correlation coefficients between independent biological replicates indicated that our RNA-seq data were consistent and reproducible (Supplementary Figure S10). We identified many more upregulated than downregulated genes in *sant-null* and *hda6* mutants under both normal and heat treatment conditions (Figure 5A and Supplementary Table S5), which is consistent with the role of the SANT domain proteins and HDA6 in transcriptional repression. In addition, more upregulated genes were specifically identified in *sant-null* than in *hda6* under both conditions (Figure 5A). The expression of most of the *sant-null* upregulated genes under normal growth conditions was also increased after heat treatment in *sant-null* and vice versa, with 510 (33%) genes reaching a significant level mutually (Figure 5B, C and D). Since *SANT1/2/3/4* mutation positively regulated plant thermotolerance, we next determined the expression of *SANT1-SANT4* genes in Col-0 before and after 37 °C treatment and found that heat treatment substantially reduced mRNA levels of all four *SANT* genes (Figure 5E, Supplementary Figure S11). In addition, we found that except

SANT3, the expression of all the other *SANT* genes was significantly higher in *hda6* than in Col-0 after 37 °C treatment (Figure 5E, Supplementary Figure S11). Conversely, the absence of SANT1/2/3/4 proteins didn't influence the expression of *HDA6* under both normal growth and heat stress conditions (Figure 5F, Supplementary Figure S11).

We then detected the transcriptional regulation of SANT1/2/3/4 and HDA6 on HI genes (heat treatment-induced upregulation of genes in Col-0 compared to that under normal growth conditions; Supplementary Table S6). Notably, 115 out of the 2109 HI genes were significantly upregulated in *sant-null* than in Col-0 after 37 °C treatment, and only 42 of the HI genes were downregulated in *sant-null* mutant (Figure 6A). In contrast, more HI genes were significantly downregulated than upregulated after 37 °C treatment in *hda6* (Figure 6A). Heatmap and boxplot analyses illustrated that these 115 genes were more markedly induced by heat treatment in *sant-null* than in Col-0 or *hda6* (Figure 6B, C). GO enrichment analysis revealed that these 115 HI genes were mainly involved in processes of transcriptional regulation, protein transport and localization and plant growth, development and metabolism (Supplementary Figure S12). Genome browser view and RT-qPCR analysis of the expression levels of representative HI genes, *HTT1*, *STRESS-ASSOCIATED PROTEIN 10* (*SAP10*), *SYNAPTOTAGMIN 4* (*SYTD*), *AT4G39360*, and *AT2G23110*, functionally annotated as heat-responsive genes according to TAIR database (https://www.arabidopsis.org/index.jsp) revealed that their expression levels were increased significantly in *sant-null* than in Col-0 and *hda6* after 37 °C treatment (Supplementary Figure S13 and Figure 6D). Notably, *sant-null*-upregulated HI genes were also upregulated under normal conditions in *sant-null* compared to those in Col-0 and *hda6* (Figure 6B, D), indicating that the transcriptionally active state of HI genes in *sant-null* mutant under normal conditions may prime the plant to quickly respond to heat stress. Although some HI genes were upregulated in *hda6* under both conditions, the lower extent of increase was probably not sufficient to enhance the plant thermotolerance (Figure 6B, D). Collectively, these results suggest that *SANT1/2/3/4* mutation contributes to the activation of HI genes, thereby improving plant thermotolerance.

H3KAc is enriched in some of the upregulated HI genes in *sant-null* mutant

We observed that high gene expression in *sant-null* or *hda6* was typically associated with high H3KAc or histone Khib level. Therefore, we examined H3KAc and histone Khib levels of *sant-null*-upregulated HI genes (115) based on our ChIP-seq data. H3KAc and histone Khib levels of the 115 genes were higher in *sant-null* than in Col-0 (Figure 7A). Moreover, 58 (50%) out of the 115 genes showed significantly higher H3KAc levels, whereas only 8 (7%) genes showed significantly higher histone Khib levels in *sant-null* mutant (Figure 7B), indicating that H3KAc increase caused by *sant-null* was more associated with HI genes activation compared to histone Khib. To verify this, we conducted H3KAc and histone Khib ChIP-qPCR assay of representative HI genes in Col-0, *sant-null*, and *hda6*. We found that the H3KAc levels, rather than histone Khib levels, were associated with gene expression levels under normal growth condition and after 37 °C treatment (Figure 7C). ChIP-seq data under normal growth condition also revealed that the H3KAc levels of representative HI genes were increased in *sant-null*, while histone Khib levels remained unchanged (Supplementary Figure S14). Notably, H3KAc levels of most of those representative HI genes were lower in *hda6* than in *sant-null* under both conditions, consistent with their relatively low expression levels in *hda6* (Figure 7C and Supplementary Figure S14). We found that SANT3-Flag was enriched at some of these 115 HI genes under normal growth condition (Supplementary Figure S15A). Snapshots of IGV clearly displayed enrichment of SANT3-Flag on three representative HI genes (Supplementary Figure S15B). ChIP-qPCR using *SANT3-Flag* transgenic seedlings detected enrichment of SANT3-Flag at representative HI genes *SAP10*, *AT4G39360* and *AT2G23110* under both normal growth condition and after 37 °C treatment (Supplementary Figure S15C). Taken together, our results revealed an underlying mechanism by which increased HI gene expression with elevated H3KAc enrichment under normal and heat treatment conditions caused by *SANT1/2/3/4* mutation leads to enhanced thermotolerance in *sant-null* mutant.

Discussion

In eukaryotic cells, histone PTMs, such as histone lysine acetylation and recently identified short-chain fatty acid acylation Khib, act as active epigenomic marks and participate in several biological processes (Shahbazian and Grunstein, 2007; Zheng et al., 2021). SANT1/2/3/4 proteins derived from *PIF/Harbinger* transposases, form a histone deacetylase complex with HDA6 in Arabidopsis (Feng et al., 2021; Zhou et al., 2021). Here, we found that SANT1/2/3/4 coordinated H3KAc and histone Khib to participate in transcriptional regulation. Moreover, SANT1/2/3/4 repressed the expression of HI genes to negatively regulate plant thermotolerance.

SANT1/2/3/4 coordinate H3KAc and histone Khib to regulate gene expression

In mammalian cells, histone acetylation dynamically competes with Khib and other acylations in highly active gene promoters (Dai et al., 2014). However, plants use a more sophisticated mechanism to avoid competition between histone acetylation and Khib and other acylations at N-tails by occupying sites free of acetylation with Khib marks (Zhang et al., 2007). In Arabidopsis, histone KAc and Khib generally act in combination, not antagonistically, to maintain high transcriptional outputs (Zheng et al., 2021). In this study, although SANT1/2/3/4 regulated H3KAc and histone Khib mostly at different regions of the genome, the relative H3KAc and histone Khib levels of *sant-null* upregulated genes were significantly higher than those of downregulated genes or of all genes, indicating that H3KAc and histone Khib regulated by SANT1/2/3/4 act in concert to repress gene expression (Figure 2 and Figure 3A). Genes gained H3KAc alone and genes gained both of the modifications in *sant-null* showed higher relative expression, but genes gained histone Khib alone in *sant-null* plants showed no obvious expression changes (Figure 3B). In addition, a small proportion of *sant-null*-upregulated genes exhibited low H3KAc levels but high histone Khib levels in *sant-null* than in Col-0 and high SANT3-Flag enrichment levels (Figure 3C, D, E and Supplementary Figure S6). Therefore, we conclude that H3KAc and histone Khib coordinated by SANT1/2/3/4 act in concert to regulate gene expression, with H3KAc playing a predominant role and Khib acting complementarily to H3KAc.

SANT1/2/3/4 negatively regulate plant thermotolerance

SANT1/2/3/4 were previously shown to form complex with HDA6, which promotes flowering by suppressing the flowering repressors, *FLOWERING LOCUS C* (*FLC*), *MADS AFFECTING FLOWERING 4* (*MAF*4), and *MAF5* (Zhou et al., 2021). Here, these *PIF*/*Harbinger* transposases derived proteins were found to be involved in heat stress regulation in plant. Surprisingly, in this study, *sant-null* and *hda6* mutants exhibited enhanced and impaired thermotolerance, respectively, after HS (Figure 4). Similar discrepancies have been reported in other studies. POWERDRESS (PWR) primarily functions as a repressor of gene expression by promoting histone deacetylation via its interaction with HDA9 (Kim et al., 2016). Interestingly, PWR and HDA9 play positive and negative roles in plant immunity, respectively, indicating that PWR-mediated plant pathogen defense is most likely independent of HDA9 activity (Yang et al., 2020; Patil et al., 2022). In addition, HIGH EXPRESSION OF OSMOTICALLY RESPONSIVE GENE 15 (HOS15) is a core member of the Arabidopsis HDA9–PWR complex and is involved in transcriptional regulation and plant development (Mayer et al., 2019; Park et al., 2019). However, HOS15 has additional functions independent of HDA9. For example, by forming complexes with PWR and HD2C, HOS15 plays a role in defining the chromatin structure at cold-regulated (*COR*) gene promoters to participate in the cold stress signaling pathway (Lim et al., 2020).

Here, we found that HI gene levels were distinctly elevated in *sant-null* mutant under both normal and heat treatment conditions, which was associated with increased H3KAc levels (Figure 6 and Figure 7). Moreover, SANT3-Flag showed an enrichment at some of the 115 *sant-null*-upregulated HI genes under normal growth condition (Supplementary Figure S15A, B), and ChIP-qPCR analysis revealed that heat stress didn't affect the enrichment of SANT3 at representative HI genes (Supplementary Figure S15C). However, HDA6-Flag showed no enrichment under normal growth condition (Supplementary Figure S15D). In order to figure out whether heat treatment affect the interaction between SANT3 and HDA6, we performed

IP-MS with *SANT3-Flag* and *HDA6-Flag* transgenic plants after heat treatment. Interestingly, SANT3 and HDA6 could be co-immunoprecipitated after heat treatment and both of them were still components of the complex we identified under normal condition (Supplementary Table S7). The findings above suggest that SANT1/2/3/4 probably regulate histone deacetylation and gene expression in both of the HDA6-dependent and independent manner after heat treatment.

We then used H3KAc ChIP-seq data and RNA-seq data under normal growth condition to illustrate the extensive role of SANT1/2/3/4 in regulation of genome-wide gene transcription. Although sites of SANT1/2/3/4- and HDA6-mediated H3KAc changes significantly overlapped, 2327 out of 2751 (85%) peaks were SANT1/2/3/4-specific (Supplementary Figure S16A). Annotation of *sant-null* and *hda6* up-H3KAc peaks revealed 2110 *sant-null*-specifically mediated up-H3KAc genes (Supplementary Table S2). In addition, expression levels of *sant-null*-specifically mediated up-H3KAc genes were increased in *sant-null*, with 247 genes being significantly upregulated, and to a much lesser extent in *hda6* compared to Col-0 (Supplementary Figure S16B, C and D), suggesting that SANT1/2/3/4 repress gene transcription by regulating histone deacetylation partially independently of HDA6 under normal growth condition.

H3Kac, not histone Khib, enriched in activated HI genes in *sant-null* mutant

In rice, histone Kbu, Kcr, and H3K9ac redundantly mark a large number of active genes. However, starvation and submergence induce changes in H3K9ac and histone Kbu/Kcr with different dynamics in different sets of genes, suggesting that these histone marks have non-redundant functions in different contexts (Lu et al., 2018). Histone lysine acylation, which is regulated by metabolism in animal cells, affects gene expression and may be functionally different from histone lysine acetylation (Sabari et al., 2017). In Arabidopsis, histone Khib is mainly enriched in genes related to sugar metabolism and phenylpropanoid biosynthesis and helps to fine-tune plant responses to dark-induced starvation (Zheng et al., 2021). In this study, SANT1/2/3/4 proteins modulated target gene transcription by coordinating histone H3KAc and

Khib modifications under normal growth condition. However, compared to histone Khib, remarkably increased H3KAc levels played a predominant role in activating HI genes expression under both normal and heat stresss conditions, leading to enhanced thermotolerance in *sant-null* mutant (Figure 7). Thus, we proposed a model in which SANT1/2/3/4 repressing the transcription of heat-inducible genes via histone deacetylation to negatively regulate plant thermotolerance (Supplementary Figure S17).

Interestingly, the HS memory regulator, *FORGETTER 2* (*FGT2*), and HS memory-related genes, *HSP17.6C*, *HSP18.2*, and *HSP21* (Urrea et al., 2020; Friedrich et al., 2021; Yamaguchi et al., 2021), were highly activated in *sant-null* than in Col-0 under normal growth conditions, consistent with their increased H3KAc levels in *sant-null* mutant (Supplementary Figure S18). This suggests that SANT1/2/3/4 participate in the regulation of HS-induced transcriptional memory. In nature, plants are frequently subjected to HS because high temperatures often recur due to climate change. Therefore, apart from the immediate HS response investigated in this study, future studies should explore the potential effects of SANT1/2/3/4 proteins on HS memory. Unravelling the regulatory mechanisms by which SANT1/2/3/4 proteins modulate plant thermotolerance could benefit crop breeding to cope with global warming.

Materials and Methods

Plant materials and growth conditions

Arabidopsis (*Arabidopsis thaliana*) accession Columbia-0 (Col-0) was used as the wild-type. EMS *hda6* allele (*axe1-5*) was obtained from the Arabidopsis Biological Resource Center. The T-DNA insertion line, *hda9* (Salk_007123), was used for Khib ChIP-seq. The higher-order *SANT* mutant, *sant-null*, complementation line, *SANT3-Flag*, in *sant-null* background and transgenic plants *HDA6-Flag* were generated in a previous study (Zhou et al., 2021).

Arabidopsis seeds were surface sterilized, sown on half-strength Murashige and Skoog (MS) medium, stratified at 4 °C for two days, and moved to a growth chamber with a long-day

photoperiod (16 h light, 22 °C/8 h darkness, 20 °C).

HS treatments

A thermotolerance assay was performed as previously described (Li et al., 2014). For phenotyping, seven-day-old seedlings were treated at 37 °C for 1 h, recovered at 22 °C for 2 h, and then treated at 44 °C for 3.5 h. We used a growth chamber to perform HS treatment. Photographs were taken, and the survival rates were measured after seven days of recovery at 22 °C. For RNA-sequencing (seq) and reverse transcription-quantitative polymerase chain reaction (RT-qPCR) and ChIP-qPCR validation, seven-day-old seedlings were treated at 37 °C for 1 h before harvesting for RNA extraction and ChIP assay. Seven-day-old seedlings grown at 22 °C were also collected as control samples.

Immunoprecipitation and mass spectrometry (IP-MS)

The affinity purification was performed according to our previous study (Zhou et al., 2021). Approximately 2 g of seven-day-old seedlings grown on half-strength MS medium after 37 °C treatment for 1 h collected from *SANT3-Flag* and *HDA6-Flag* transgenic plants or wild-type plants were used for affinity purification. Following centrifugation, the supernatant was incubated with 10 μg of anti-Flag (F1804; Sigma) antibody and 100 μl of Dynabeads Protein G (10003D; Invitrogen) for 3 h at 4°C with rotation. Beads were then washed three times with lysis buffer and three times with wash buffer (150 mM NaCl, 50 mM Tris-HCl pH 8.0, 5 mM $MgCl_2$). Immunoprecipitated proteins were run on a 10% SDS-PAGE gel and subjected to liquid chromatography tandem mass spectrometry (LC-MS/MS) analysis.

RNA-seq and data analysis

Triplicate samples of Col-0, *sant-null*, and *hda6* plants were collected for RNA-seq analysis. Total RNA was extracted from seven-day-old seedlings with and without 37 °C treatment using the TRIzol reagent (Invitrogen) and sent to Novogene Co., Ltd. (Beijing, China) for library preparation and transcriptome sequencing. Libraries were prepared using the

NEBNext Ultra RNA Library Prep Kit (Illumina, NEB, USA) and sequenced on an Illumina NovaSeq 6000 platform, according to the manufacturer's instructions. The sequenced raw data were trimmed using Trim Galore v.0.6.6 to remove the adapter sequences and low-quality reads. The remaining clean reads were mapped to the TAIR10 Arabidopsis reference genome using Hisat2 v. 2.2.1. Only uniquely mapped reads were retained for subsequent analysis and visualized using the Integrative Genomics Viewer (IGV). Gene expression levels were estimated using featureCounts v.2.0.1. Differentially expressed genes were determined using the R package DESeq2 v.1.30.1, where *P*-value < 0.05 and $|\log_2$(fold change)| > 1were considered significant. The expression level of each gene was expressed as fragments per kilobase per million mapped reads. Heatmaps and boxplots showing the gene expression levels were generated in R. Gene ontology (GO) enrichment analysis was performed using the R package *clusterProfiler* in Bioconductor.

Chromatin immunoprecipitation (ChIP)

ChIP was performed as previously described (Zhou et al., 2021). Approximately 2 g of seedlings grown on half-strength MS medium at 22 °C or at 37 °C for 1 h was collected, fixed with 1% (v/v) formaldehyde for 15 min, and ground into a powder in liquid nitrogen. Nuclei were isolated and chromatin was fragmented to 200–500 bp via sonication with a Bioruptor (Diagenode). After centrifugation, the sonicated chromatin was incubated with Pan-anti-Khib (PTM-802; PTM Bio-labs, Hangzhou, China), anti-acetylated Histone H3 (06-599; Merck Millipore) and anti-Flag (F1804; Sigma) antibody overnight and incubated with Dynabeads Protein G (10003D; Invitrogen) for 2 h with agitation at 4 °C. Precipitated chromatin was washed and eluted with the elution buffer (0.5% (w/v) SDS and 0.1 M $NaHCO_3$) and concentrated via phenol–chloroform extraction and ethanol precipitation. Precipitated and input DNA samples were subjected to qPCR or sequencing.

ChIP-seq and data analysis

For histone Khib ChIP-seq, two biological replicates for input and immunoprecipitated DNA

of Col-0, *sant-null*, *hda6*, and *hda9* were sent to Novogene Co., Ltd. (Beijing, China) for library construction and sequencing (150-bp pair-end reads; Illumina NovaSeq 6000). Adapter sequences and low-quality reads were removed from the raw data using Trim Galore v.0.6.6. The resulting high-quality reads were mapped to the TAIR10 Arabidopsis reference genome using Bowtie2 v.2.2.5 with default parameters. PCR duplicates were removed using Sambamba v.0.6.6, and uniquely mapped reads were retained for further analysis and visualized using IGV (Langmead and Salzberg, 2012; Tarasov et al., 2015). Enriched ChIP and differentially enriched peaks between mutants and wild type were determined using program SICER2 v.1.0.3 with the following parameters: "redundancy threshold=1; window size = 200; effective genome fraction = 0.85; gap size = 200; and FDR = 0.05". Peaks with FDR < 0.05 and fold change of mutants/Col-0 ≥ 1.25 were considered as significant up-Khib peaks and annotated with Arabidopsis genome using the intersect function in BEDTools suite. Metaplots and heat maps illustrating the ChIP-seq data were plotted using deepTools. Then, H3KAc ChIP-seq and RNA-seq data from our previous study (Zhou et al., 2021) combined with the Khib ChIP-seq data from this study were used to conduct integrative analysis. The read count of each gene region and overlap analysis of H3KAc or histone Khib peaks were performed using the intersect function in BEDTools suite. The histone Khib level of each gene was given as reads per kilobase per million mapped reads. Heatmaps and boxplots showing histone Khib levels were generated in R. The simulation region, randomly selected from the whole genome with the same length distribution of peaks, was generated using the shuffle function in BEDTools suite.

RT-qPCR and ChIP-qPCR analysis

For RT-qPCR, total RNA was extracted from Arabidopsis seedlings with or without 37 °C treatment using the TRIzol reagent (Invitrogen) and treated with DNase I (Takara) to remove genomic DNA contaminants. Total RNA was reverse-transcribed into cDNA using the PrimeScript RT Reagent Kit (RR047A; Takara). ChIP-qPCR was performed using immunoprecipitated and input DNA samples. Real-time quantitative PCR was performed on a

CFX96 Real-Time PCR system (Bio-Rad) using ChamQ Universal SYBR qPCR Master Mix (Vazyme). *ACT2* was used as an internal control for RT-qPCR. Three biological replicates were used for real-time PCR, with three technical replicates per biological replicate. All primers used in this study are listed in Supplementary Table S8.

Statistical analyses

P-values in overlap analyses were calculated by hypergeometric distribution using the R package GeneOverlap v.1.26.0. The levels of significance (*P*-value) such as differences of gene expression, H3KAc and Khib levels between each sample were measured using R statistical software.

Accession numbers

The accession nos. for genes are as follows: *SANT1* (AT1G09050), *SANT2* (AT1G09040), *SANT3* (AT2G47820), *SANT4* (AT1G55050), *HDA6* (AT5G63110), and *HDA9* (AT3G44680). High-throughput sequencing data were deposited in the Gene Expression Omnibus database under accession no. GSE243707.

Supplementary Data

Supplementary Figure S1. Histone deacetylase HDA6 and SANT domain-containing proteins (SANT1/2/3/4) co-regulate histone 2-hydroxyisobutyrylation (Khib) modification.

Supplementary Figure S2. Histone deacetylase HDA9 and SANT1/2/3/4 co-regulate histone Khib modification.

Supplementary Figure S3. Gene Ontology (GO) term enrichment analysis of 291 genes with increased histone Khib in *sant-null*, *hda6* and *hda9* mutants.

Supplementary Figure S4. SANT1/2/3/4 proteins localize to specific sites of the genome to regulate histone Khib modifications and gene expressions.

Supplementary Figure S5. RT-qPCR and ChIP-qPCR validation of expression levels (left) and histone Khib levels (right) in Col-0 and *sant-null* at four representative gene regions displayed in Supplementary Figure S4B.

Supplementary Figure S6. Metaplots of normalized SANT3-Flag enrichment levels in Col-0 and *SANT3-Flag* transgenic plants at *sant-null* upregulated gene regions with H3KAc levels reduced (138, left) and random genes (right).

Supplementary Figure S7. RT-qPCR and ChIP-qPCR validation of expression levels (left), H3KAc levels (middle) and histone Khib levels (right) in Col-0 and *sant-null* at two representative gene regions displayed in Figure 3E.

Supplementary Figure S8. Snapshots of the genome browser illustrating the expression levels of *HEAT-INDUCED TAS1 TARGET 1* (*HTT1*) and *HTT4* in Col-0, *sant-null*, and *hda6* under normal growth conditions.

Supplementary Figure S9. Phenotypic analysis (A) and Fresh weight (B) of Col-0, *sant-null*, and *hda6* seedlings grown on 1/2 Murashige and Skoog (MS) medium under normal growth conditions after 7 days.

Supplementary Figure S10. Heatmap showing the spearman correlation coefficient among each sample of Col-0, *sant-null*, and *hda6* with three biological replicates from RNA-sequencing (seq) data.

Supplementary Figure S11. RT-qPCR validation of expression levels of *SANT1/2/3/4* (left) and *HDA6* (right) under normal growth conditions and after 37°C treatment.

Supplementary Figure S12. Gene Ontology (GO) term enrichment analysis of 115 *sant-null*-upregulated HI genes.

Supplementary Figure S13. Snapshots of the genome browser illustrating the expression levels of representative heat-inducible genes in Col-0, *sant-null*, and *hda6* under normal growth conditions and after 37°C treatment.

Supplementary Figure S14. H3KAc (left) and histone Khib (right) enrichment levels of representative HI genes in Col-0, *sant-null*, and *hda6* under normal growth condition.

Supplementary Figure S15. SANT3-Flag was enriched at some of the HI genes.

Supplementary Figure S16. SANT1/2/3/4 regulate gene expression by mediating H3KAc partially independent of HDA6.

Supplementary Figure S17. Working model of SANT1/2/3/4 negatively regulating heat tolerance in Arabidopsis.

Supplementary Figure S18. Snapshots of the genome browser illustrating the expression and H3Kac levels of heat stress memory regulator *FGT2* and heat stress memory-related genes, *HSP17.6C*, *HSP18.2*, and *HSP21* in Col-0 and *sant-null* under normal growth conditions.

Supplementary Table S1. List of high levels of histone 2-hydroxyisobutyrylation (Khib) peaks in *sant-null*, *hda6*, and *hda9.*

Supplementary Table S2. Annotated gene list of up-H3KAc or up-Khib peaks in the indicated mutants.

Supplementary Table S3. Histone Khib levels of *sant-null*-, *hda6*-, and *hda9*-upregulated genes.

Supplementary Table S4. List of differentially expressed genes in *hda9*.

Supplementary Table S5. List of differentially expressed genes in *sant-null* and *hda6* under normal conditions and after 37°C treatment.

Supplementary Table S6. List of heat-inducible (HI) genes.

Supplementary Table S7. List of proteins co-immunoprecipitating with SANT3 and HDA6. The interacting proteins were affinity-purified and analyzed by mass spectrometry.

Supplementary Table S8. List of primers used in this study.

Funding

This work was supported by the National Natural Science Foundation of China (32170610), the GuangDong Basic and Applied Basic Research Foundation (2022A1515111040), and the Science, Technology and Innovation Commission of Shenzhen Municipality.

Acknowledgments

We would like to thank Prof. Daoxiu Zhou of Huazhong Agricultural University, Wuhan, Hubei, China for providing *hda9* (Salk_007123) seeds used in this study.

Author contributions

XS Z and CJ Z designed and conceived the study. XS Z, YJ F, XY Z, JN H, PF L, and SP S performed the experiments. XS Z, J G, JK Z, and CJ Z analyzed the data and wrote the manuscript. All authors discussed the results and reviewed the manuscript before submission.

Declaration of interests

The authors declare no competing interests.

Figure legends

Figure 1. SANT domain-containing proteins (SANT1/2/3/4) co-regulate histone 2-hydroxyisobutyrylation (Khib) with histone deacetylase HDA6 or HDA9 to repress gene expression. **A)** Metaplots and heatmaps showing Khib enrichment level at 2 kb surrounding *sant-null* up-Khib peaks in Col-0, *sant-null*, *hda6* and *hda9*. Color scale indicates normalized reads per kilobase per million mapped reads (RPKM) values. **B)** Venn diagram showing the overlap of *sant-null*-, *hda6*-, and *hda9*-mediated up-Khib genes. **C)** Venn diagram showing the overlap of *sant-null*-mediated up-Khib genes and *sant-null*-upregulated or downregulated genes. **D)** Boxplot showing the relative histone Khib enrichment levels (*sant-null*/Col-0) of *sant-null*-mediated up-Khib genes with significantly higher expression levels in *sant-null* (103) and all the remaining *sant-null*-mediated up-Khib genes (2268). **E)** Boxplot (left) and metaplot (right) of normalized histone Khib enrichment level (RPKM) in Col-0, *sant-null*, *hda6*, and *hda9* at regions of *sant-null*-upregulated genes (1047). –2 Kb and 2 Kb in metaplot represent 2 Kb upstream of the transcription start site (TSS) and 2 Kb downstream of the transcription end site (TES). Boxplots of D) and E) show maximum, third quartile, median, first quartile and minimum from top to bottom. *P*-values in overlap analyses were calculated using a

hypergeometric distribution. Asterisks (**) indicate the significant differences at $P < 0.01$ (two-sided Wilcoxon rank sum tests).

Figure 2. SANT1/2/3/4 regulate H3KAc and histone Khib modifications mostly in different regions of Arabidopsis genome. **A)** Venn diagram showing the overlap of H3KAc and Khib peaks in Col-0. Because of different length of peaks, one peak of Khib likely overlaps with two or more H3KAc peaks and vice versa. '11807/10174' indicates numbers of Khib and H3KAc peaks in Col-0, respectively. **B)** Venn diagram showing the overlap of peaks with higher H3KAc and histone Khib levels in *sant-null* than in Col-0. '122/128' indicates numbers of *sant-null* up Khib and *sant-null* up H3KAc peaks, respectively. **C)** Venn diagram showing the overlap of *sant-null*-mediated up-H3KAc and up-Khib genes. **D)** Metaplots and heatmaps of H3KAc enrichment level in 2 kb surrounding *sant-null* up-Khib peaks (left) and simulation region (right) in Col-0 and *sant-null*. Simulation region is included as a control region. Color scale indicates the normalized RPKM values. **E)** Metaplots and heatmaps of histone Khib enrichment level in 2 kb surrounding *sant-null* up-H3Kac peaks (left) and simulation region (right) in Col-0 and *sant-null.* Simulation region is included as a control region. Color scale indicates the normalized RPKM values. *P*-values in overlap analyses were calculated using the hypergeometric distribution.

Figure 3. SANT1/2/3/4 regulate gene expression by coordinating histone H3KAc and Khib modifications. **A)** Boxplot showing relative H3KAc and Khib enrichment levels (*sant-null*/Col-0) of upregulated (1047), downregulated (317), and all genes (32538) in *sant-null*. **B)** Boxplot showing the relative expression levels (*sant-null*/Col-0) of different group of genes: gained H3KAc alone (2310), gained Khib alone (2179), gained both H3KAc and Khib in *sant-null* (192), and all genes in the genome (32538). Each box represents the fragments per kilobase per million mapped reads (FPKM) values. **C and D**) Heatmap (C) and boxplot (D) illustrating the H3KAc and Khib enrichment levels in Col-0 and *sant-null*, with *sant-null* upregulated genes and H3KAc levels reduced in *sant-null* (138). Color scale of

heatmap and each box of boxplot indicate the normalized RPKM values. **E)** Snapshots of the genome browser illustrating the expression and H3KAc and Khib levels at two representative loci in Col-0 and *sant-null*. Boxplots of A) , B) and D) show maximum, third quartile, median, first quartile and minimum from top to bottom. Asterisks (* and **) indicate the significant differences at $P < 0.05$ and $P < 0.01$, respectively (two-sided Wilcoxon rank sum tests).

Figure 4. SANT1/2/3/4 negatively regulate plant thermotolerance. **A)** Phenotypic analysis of Col-0, *sant-null*, and *hda6* seedlings grown on 1/2 Murashige and Skoog (MS) medium under normal growth conditions (left) or after heat stress (HS) treatment (right). Schematic representation of the temperature conditions used for the thermotolerance assay in this study on the top. **B)** Survival rates of seedlings shown in (A). Data are presented as the mean ± standard deviation (SD) of eight biological replicates. **C)** Phenotypic analysis of Col-0, *sant-null*, and the complementation line *SANT3-Flag* grown on 1/2 MS medium under normal growth conditions (left) or after HS treatment (right). **D)** Survival rates of seedlings shown in (C). Data are presented as the mean ± SD of eight biological replicates. Asterisks (**) indicate the significant differences at $P < 0.01$, and 'ns' indicates no significant differences (Student's t tests).

Figure 5. Transcriptome profiling of *sant-null* and *hda6* compared to Col-0 under normal growth conditions and after 37 ℃ treatment. **A)** Number of differentially expressed genes in *sant-null* and *hda6* compared to Col-0 under normal growth conditions and after 37 ℃ treatment ($P < 0.05$ and a two-fold cutoff were used). **B)** Venn diagram showing the overlap of upregulated genes under normal growth conditions and after 37 ℃ treatment in *sant-null* compared with Col-0. *P*-value was calculated using the hypergeometric distribution. **C and D)** Heatmap illustrating the expression levels of *sant-null*-upregulated genes under normal growth conditions (C) and after 37 ℃ treatment (D) in the indicated materials. Color scale indicates the normalized FPKM (fragments per kilobase per million mapped reads) values. **E)** Expression levels of *SANT1/2/3/4* in Col-0 and *hda6* under normal growth conditions and after 37 ℃

treatment based on RNA-sequencing (seq) data. **F)** Expression levels of *HDA6* in Col-0 and *sant-null* under normal growth conditions and after 37 ℃ treatment based on RNA-seq data. Data are presented as the mean ± SD of three biological replicates. Asterisks (*) indicate the significant differences at $P < 0.05$, and 'ns' indicates no significant differences (Student's t tests).

Figure 6. Expression levels of heat-inducible (HI) genes increase significantly in *sant-null* mutant. **A)** Venn diagram showing the overlap of HI genes in Col-0 and *sant-null* (up)- or *hda6* (down)-mediated differently expressed genes after 37 ℃ treatment. **B)** Heatmap illustrating the expression levels of *sant-null*-upregulated HI genes (115) in Col-0, *sant-null*, and *hda6* under normal growth conditions and after 37 ℃ treatment. Color scale indicates the normalized FPKM values. **C)** Boxplot showing the relative expression levels (37/22 ℃) of *sant-null*-upregulated HI genes (115) in Col-0, *sant-null*, and *hda6*. Boxplot shows maximum, third quartile, median, first quartile and minimum from top to bottom. Asterisks (**) indicate the significant differences at $P < 0.01$ (two-sided Wilcoxon rank sum tests). **D)** Reverse transcription-quantitative polymerase chain reaction (RT-qPCR) validation of the expression levels of representative HI genes in Col-0, *sant-null*, and *hda6* under normal growth conditions and after 37 ℃ treatment. *ACT2* was used as an internal control. Error bars indicate the standard deviation of three biological replicates. Asterisks (* and **) indicate the significant differences at $P < 0.05$ and $P < 0.01$, respectively (Student's t tests).

Figure 7. Histone H3KAc is enriched in some of the upregulated HI genes in *sant-null* mutant. **A)** Heatmap showing the H3KAc and histone khib enrichment levels of *sant-null* upregulated HI genes (115) in Col-0 and *sant-null* under normal growth conditions. Color scale indicates the normalized RPKM (reads per kilobase per million mapped reads) values. **B)** Venn diagram showing the overlap of *sant-null*-upregulated HI genes and *sant-null*-mediated up-H3KAc (up) or up-Khib (down) genes. *P*-values were calculated using the hypergeometric distribution. **C)** H3KAc (left) and histone Khib (right) enrichment levels of representative HI genes detected by

ChIP-qPCR in Col-0, *sant-null*, and *hda6* after 37 ℃ treatment (up) and under normal growth condition (down). Error bars indicate the standard deviation of three biological replicates. Asterisks (* and **) indicate the significant differences at $P < 0.05$ and $P < 0.01$, respectively, and 'ns' indicates no significant differences (Student's t tests).

References

Allfrey, VG., Faulkner, R., and Mirsky, A. (1964). Acetylation and methylation of histones and their possible role in the regulation of RNA synthesis. *Proceedings of the National Academy of Sciences, USA* **51**(5): 786-794.

Bourgine, B., and Guihur, A. (2021). Heat shock signaling in land plants: from plasma membrane sensing to the transcription of small heat shock proteins. *Frontiers in Plant Science* **12**: 710801.

Chen, Y., Sprung, R., Tang, Y., Ball, H., Sangras, B., Kim, SC., Falck, JR., Peng, J., Gu, W., and Zhao, Y. (2007). Lysine propionylation and butyrylation are novel post-translational modifications in histones. *Molecular & Cellular Proteomics* **6** (5): 812–819.

Dai, L., Peng, C., Montellier, E., Lu, Z., Chen, Y., Ishii, H., Debernardi, A., Buchou, T., Rousseaux, S., Jin, F., et al. (2014). Lysine 2-hydroxyisobutyrylation is a widely distributed active histone mark. *Nature Chemical Biology* **10** (5): 365-370.

Duan, CG., Wang, X., Xie, S., Pan, L., Miki, D., Tang, K., Hsu, CC., Lei, M., Zhong, Y., Hou, YJ., et al. (2017). A pair of transposon-derived proteins function in a histone acetyltransferase complex for active DNA demethylation. *Cell Research*. **27**(2): 226-240.

Feng, C., Cai, X., Su, Y., L, L., Chen, S., and He, X. (2021). Arabidopsis RPD3-like histone deacetylases form multiple complexes involved in stress response. *Journal of Genetics and Genomics* **48** (5): 369-383.

Friedrich, T., Oberkofler, V., Trindade, I., Altmann, S., Brzezinka, K., Lämke, J., Gorka, M., Kappel, C., Sokolowska, E., Skirycz, A,. et al. (2021). Heteromeric HSFA2/HSFA3 complexes drive transcriptional memory after heat stress in Arabidopsis. *Nat Communications* **12** (1):3426.

Garcia, BA., Shabanowitz, J., and Hunt, DF. (2007). Characterization of histones and their post-translational modifications by mass spectrometry. *Current Opinion in Chemical Biology* **11**(1): 66-73.

He, Y., and Li, Z. (2018). Epigenetic environmental memories in plants: establishment, maintenance, reprogramming. *Trends in Genetics* **34** (11): 856–866.

Hu, Y., Lu, Y., Zhao, Y., and Zhou, DX. (2019). Histone acetylation dynamics integrates metabolic activity to regulate plant response to stress. *Frontiers in Plant Science* **10**: 1236.

Hu. Z., Song, N., Zheng, M., Liu, X., Liu, Z., Xing, J., Ma, J., Guo, W., Yao, Y., Peng, H., et al. (2015). Histone acetyltransferase GCN5 is essential for heat stress-responsive gene activation and thermotolerance in Arabidopsis. *The Plant Journal* **84**(6): 1178–1191.

Huang, H., Luo, Z., Qi, S., Huang, J., Xu, P., Wang, X., Gao, L., Li, F., Wang, J., Zhao, W., et al. (2018). Landscape of the regulatory elements for lysine 2-hydroxyisobutyrylation pathway. *Cell Research* **28**(1): 111-125.

Huang, J., Luo, Z., Ying, W., Cao, Q., Huang, H., Dong, J., Wu, Q., Zhao, Y., Qian, X., and Dai, J. (2017). 2-Hydroxyisobutyrylation on histone H4K8 is regulated by glucose homeostasis in Saccharomyces cerevisiae. *Proceedings of the National Academy of Sciences, USA* **114** (33): 8782-8787.

Kapitonov, VV., and Jurka, J. (2004). *Harbinger* transposons and an ancient *HARBI1* gene derived from a transposase. *DNA and Cell Biology*. **23**(5): 311-324.

Kebede, AF., Nieborak, A., Shahidian, LZ., Le, Gras S., Richter, F., Gómez, DA., Baltissen, MP., Meszaros, G., Magliarelli, HF., Taudt, A., et al. (2017). Histone propionylation is a mark of active chromatin. *Nature Structural & Molecular Biology* **24** (12): 1048-1056.

Kim, YJ., Wang, R., Gao, L., Li, D., Xu, C., Mang, H., Jeon, J., Chen, X., Zhong, X., Kwak, JM., et al. (2016). Powerdress and HDA9 interact and promote histone H3 deacetylation at specific genomic sites in Arabidopsis. *Proceedings of the National Academy of Sciences, USA* **113**(51):14858–14863.

Langmead, B., and Salzberg, SL. (2012). Fast gapped-read alignment with Bowtie 2. *Nature Methods* **9** (4): 357-359.

Li, S., Liu, J., Liu, Z., Li, X., Wu, F., and He, Y. (2014)**.** HEAT-INDUCED TAS1 TARGET1 mediates thermotolerance via HEAT STRESS TRANSCRIPTION FACTOR A1a-directed pathways in Arabidopsis. *The Plant Cell* **26**(4):1764-1780.

Liang, SC., Hartwig, B., Perera, P., Mora-García, S., Leau, E.d., Thornton, H., Alves, F.d.L., Rappsilber, J., Yang, S., James, GV., et al. (2015). Kicking against the PRCs- A Domesticated Transposase Antagonises Silencing Mediated by Polycomb Group Proteins and Is an Accessory Component of Polycomb Repressive Complex 2. *PLOS Genetics* **11**(12): e1005660.

Lim, CJ., Park, J., Shen, M., Park, HJ., Cheong, MS., Park, KS., Baek, D., Bae, MJ., Ali, A., Jan, M., et al. (2020). The Histone-Modifying Complex PWR/HOS15/HD2C Epigenetically Regulates Cold Tolerance. *Plant Physiology* **184** (2):1097-1111.

Lu, Y., Xu, Q., Liu, Y., Yu, Y., Cheng, ZY., Zhao, Y., and Zhou, DX. (2018)**.** Dynamics and functional interplay of histone lysine butyrylation, crotonylation, and acetylation in rice under starvation and submergence. *Genome Biology* **19** (1): 144.

Mayer, KS., Chen, X., Sanders, D., Chen, J., Jiang, J., Nguyen, P., Scalf, M., Smith, LM., and Zhong, X. (2019). HDA9-PWR-HOS15 is a core histone deacetylase complex regulating transcription and development. *Plant Physiology* **180** (1): 342–355.

Niu, Y., Bai, J., Liu, X., Zhang, H., Bao, J., Zhao, W., Hou, Y., Deng, X., Yang, C., Guo, L., et al. (2022). HISTONE DEACETYLASE 9 transduces heat signal in plant cells. *Proceedings of the National Academy of Sciences, USA* **119**(45) :e2206846119.

Park, HJ., Baek, D., Cha, JY., Liao, X., Kang, SH., McClung, CR., Lee, SY., Yun, DJ., and Kim, WY. (2019). HOS15 interacts with the histone deacetylase HDA9 and the evening complex to epigenetically regulate the floral activator GI- GANTEA. *The Plant*

Cell **31**(1): 37–51.

Patil, V., and Nandi, AK. (2022). POWERDRESS positively regulates systemic acquired resistance in Arabidopsis. *Plant Cell Reports* **41**(12):2351-2362.

Perrella, G., Baurle, I., and Zanten, M.v. (2022). Epigenetic regulation of thermomorphogenesis and heat stress tolerance. *New Phytologist* **234** (4): 1144–1160.

Sabari, BR., Zhang, D., Allis, CD., and Zhao, Y. (2017). Metabolic regulation of gene expression through histone acylations. *Nature Reviews Molecular Cell Biology* **18** (2):90–101.

Shahbazian, MD., and Grunstein, M. (2007)**.** Functions of site-specific histone acetylation and deacetylation. *Annual Review of Biochemistry* **76**: 75-100.

Tarasov, A., Vilella, AJ., Cuppen, E., Nijman, IJ., and Prins, P. (2015). Sambamba: fast processing of NGS alignment formats. *Bioinformatics* **31**(12): 2032-2034.

Castellanos, R.U., Friedrich, T., Petrovic, N., Altmann, S., Brzezinka, K., Gorka, M., Graf, A., and Bäurle, I. (2020)**.** FORGETTER2 protein phosphatase and phospholipase d modulate heat stress memory in Arabidopsis. *The Plant Journal* **104** (1), 7–17.

Velanis, CN., Perera, P., Thomson, B., Leau, E.d., Liang, S.C., Hartwig, B., Förderer, A., Thornton, H., Arede, P., Chen, J., et al. (2020). The domesticated transposase ALP2 mediates formation of a novel Polycomb protein complex by direct interaction with MSI1, a core subunit of Polycomb Repressive Complex 2 (PRC2). *PLOS Genetics* **16**(5): e1008681.

Wang, S., Wang, M., Ichino, L., Boone, BA., Zhong, Z., Papareddy, RK., Lin, EK., Yun, J., Feng, S., and Jacobsen, SE. (2024). MBD2 couples DNA methylation to transposable element silencing during male gametogenesis. *Nature Plants* **10** (1):13-24.

Wang, Y., Hu, Q., Wu, Z., Wang, H., Han, S., Jin, Y., Zhou, J., Zhang, Z., Jiang, J., Shen, Y., et al. (2017)**.** HISTONE DEACETYLASE 6 represses pathogen defence responses in *Arabidopsis thaliana*. *Plant, Cell & Environment* **40** (12):2972–2986.

Yamaguchi, N., Matsubara, S., Yoshimizu, K., Seki, M., Hamada, K., Kamitani, M., Kurita, Y., Nomura, Y., Nagashima, K., Inagaki, S., et al. (2021). H3K27me3 demethylases alter *HSP22* and *HSP17.6C* expression in response to recurring heat in Arabidopsis. *Nature Communications* **12**(1):3480.

Yang, F., Sun, Y., Du, X., Chu, Z., Zhong, X., and Chen, X. (2023)**.** Plant-specific histone deacetylases associate with ARGONAUTE4 to promote heterochromatin stabilization and plant heat tolerance. *New Phytologist* **238**(1):252-269.

Yang, L., Chen, X., Wang, Z., Sun, Q., Hong, A., Zhang, A., Zhong, X., and Hua, J. (2020). HOS15 and HDA9 negatively regulate immunity through histone deacetylation of intracellular immune receptor NLR genes in Arabidopsis. *New Phytologist* **226** (2): 507–522.

Yruela, I., Moreno-Yruela, C., and Olsen, C.A. (2021). Zn^{2+}-Dependent histone deacetylases in plants: structure and evolution. *Trends in Plant Science* **26** (7):741-757.

Yu, G., Wang, LG., Han, Y., and He, QY. (2012)**.** clusterProfiler: an R package for comparing biological themes among gene clusters. *Omics* **16**(5):284-287.

Yu, Z., Ni, J., Sheng, W., Wang, Z., and Wu, Y. (2017). Proteome-wide identification of lysine 2-hydroxyisobutyrylation reveals conserved and novel histone modifications in

Physcomitrella patens. *Scientific Reports* **7**(1):15553.

Zhang, K., Sridhar, V.V., Zhu, J., Kapoor, A., and Zhu, JK. (2007). Distinctive core histone post-translational modification patterns in *Arabidopsis thaliana*. *PLOS ONE* **2**(11): e1210.

Zhang, N., Zhang, L., Li, L., Geng, J., Zhao, L., Ren, Y., Dong, Z., and Chen, F. (2022). Global Profiling of 2-hydroxyisobutyrylome in Common Wheat. *Genomics, Proteomics & Bioinformatics* **20**(4):688-701.

Zhang, X., Jiang, N., Feschotte, C., and Wessler, S.R. (2004). PIF- and Pong-like transposable elements: distribution, evolution and relationship with Tourist-like miniature inverted-repeat transposable elements. *Genetics* **166** (2): 971-986.

Zhao, T., Zhan, Z., and Jiang, D. (2019). Histone modifications and their regulatory roles in plant development and environmental memory. *Journal of Genetics and Genomics* **46** (10): 467-476.

Zheng, L., Li, C., Ma, X., Zhou, H., Liu, Y., Wang, P., Yang, H., Tamada, Y., Huang, J., Wang, C., et al. (2021)**.** Functional interplay of histone lysine 2-hydroxyisobutyrylation and acetylation in Arabidopsis under dark-induced starvation. *Nucleic Acids Research* **49**(13) : 7347-7360.

Zhou, X., He, J., Velanis, C.N., Zhu, Y., He, Y., Tang, K., Zhu, M., Graser, L., Leau, E.d., Wang, X., et al. (2021). A domesticated *Harbinger* transposase forms a complex with HDA6 and promotes histone H3 deacetylation at genes but not TEs in Arabidopsis. *Journal of Integrative Plant Biology* **63**(8): 1462–1474.

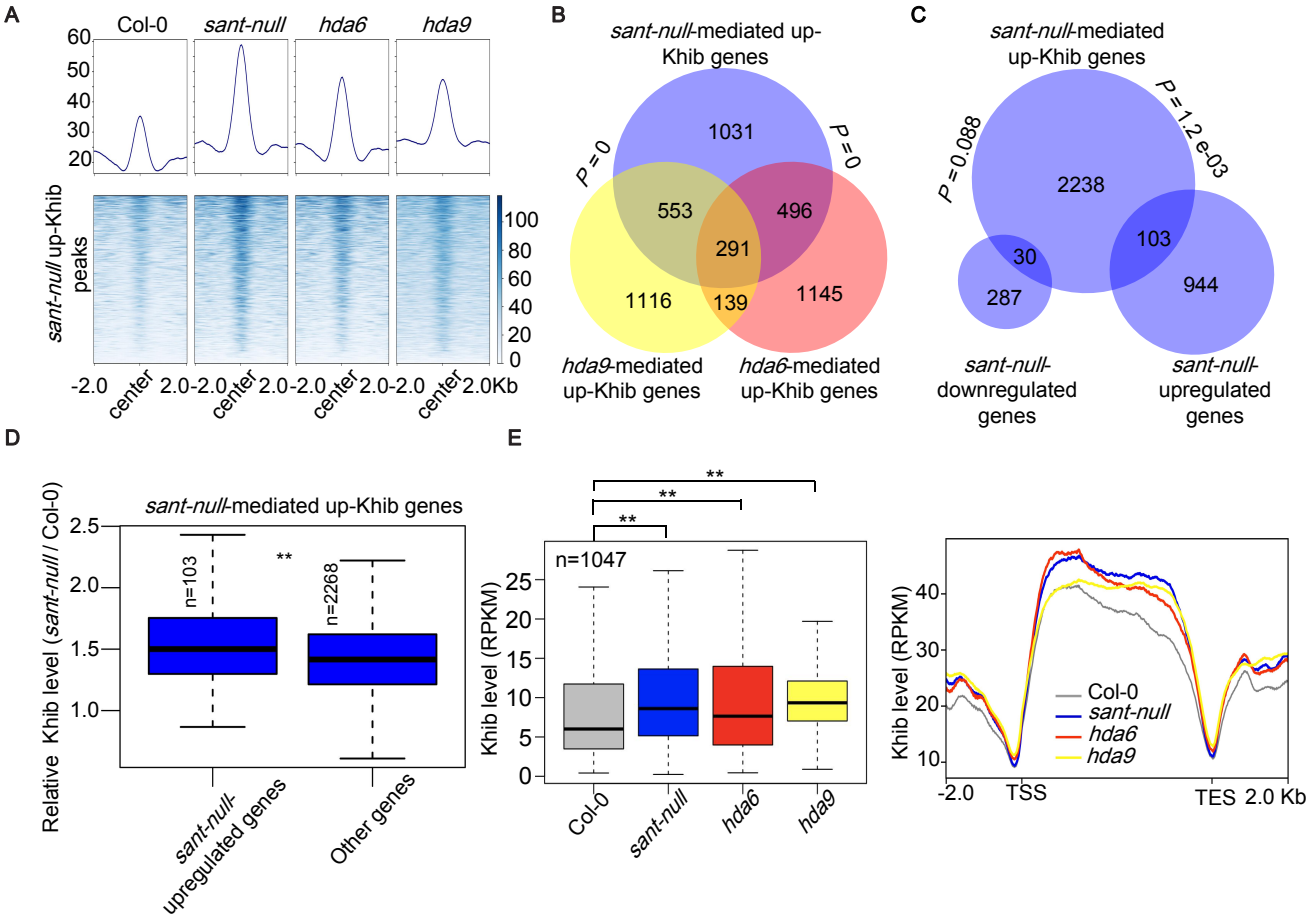
A
Col-0
sant-null
hda6
hda9
60
50
40
30
20
sant-null up-Khib peaks
100
80
60
40
20
0
-2.0
center
2.0-2.0
center
2.0-2.0
center
2.0-2.0
center
2.0Kb
B
sant-null-mediated up-Khib genes
1031
P=0
P=0
553
496
291
1116
139
1145
hda9-mediated up-Khib genes
hda6-mediated up-Khib genes
C
sant-null-mediated up-Khib genes
P=0.088
P=1.2e-03
2238
30
103
287
944
sant-null-downregulated genes
sant-null-upregulated genes
D
sant-null-mediated up-Khib genes
Relative Khib level (sant-null / Col-0)
2.5
2.0
1.5
1.0
n=103
**
n=2268
sant-null-upregulated genes
Other genes
E
**
**
**
n=1047
Khib level (RPKM)
25
20
15
10
5
0
Col-0
sant-null
hda6
hda9
Khib level (RPKM)
40
30
20
10
Col-0
sant-null
hda6
hda9
-2.0
TSS
TES
2.0 Kb

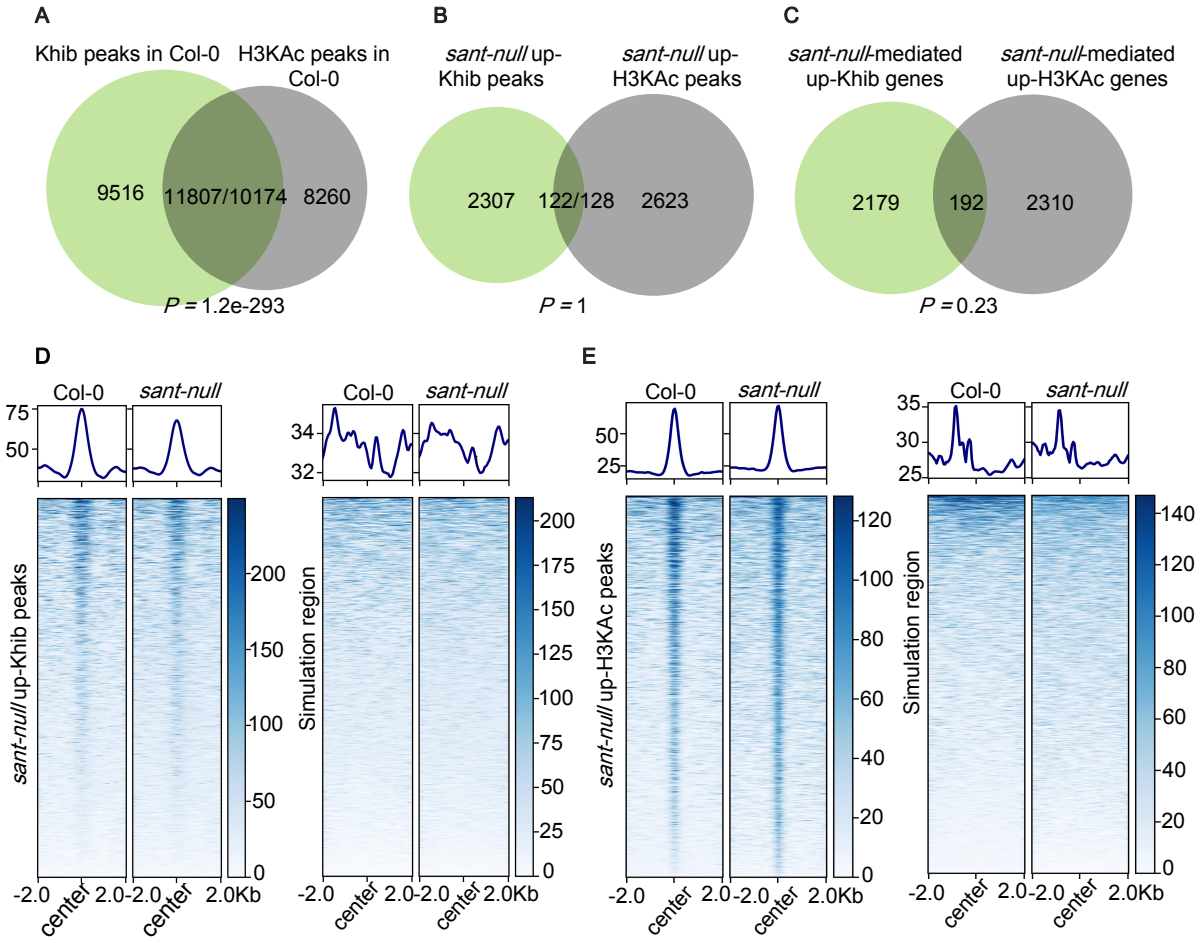
A
Khib peaks in Col-0
H3KAc peaks in Col-0
9516
11807/10174
8260
P = 1.2e-293
B
sant-null up-Khib peaks
sant-null up-H3KAc peaks
2307
122/128
2623
P = 1
C
sant-null-mediated up-Khib genes
sant-null-mediated up-H3KAc genes
2179
192
2310
P = 0.23
D
Col-0
sant-null
sant-null up-Khib peaks
Simulation region
-2.0
center
2.0
2.0Kb
E
sant-null up-H3KAc peaks

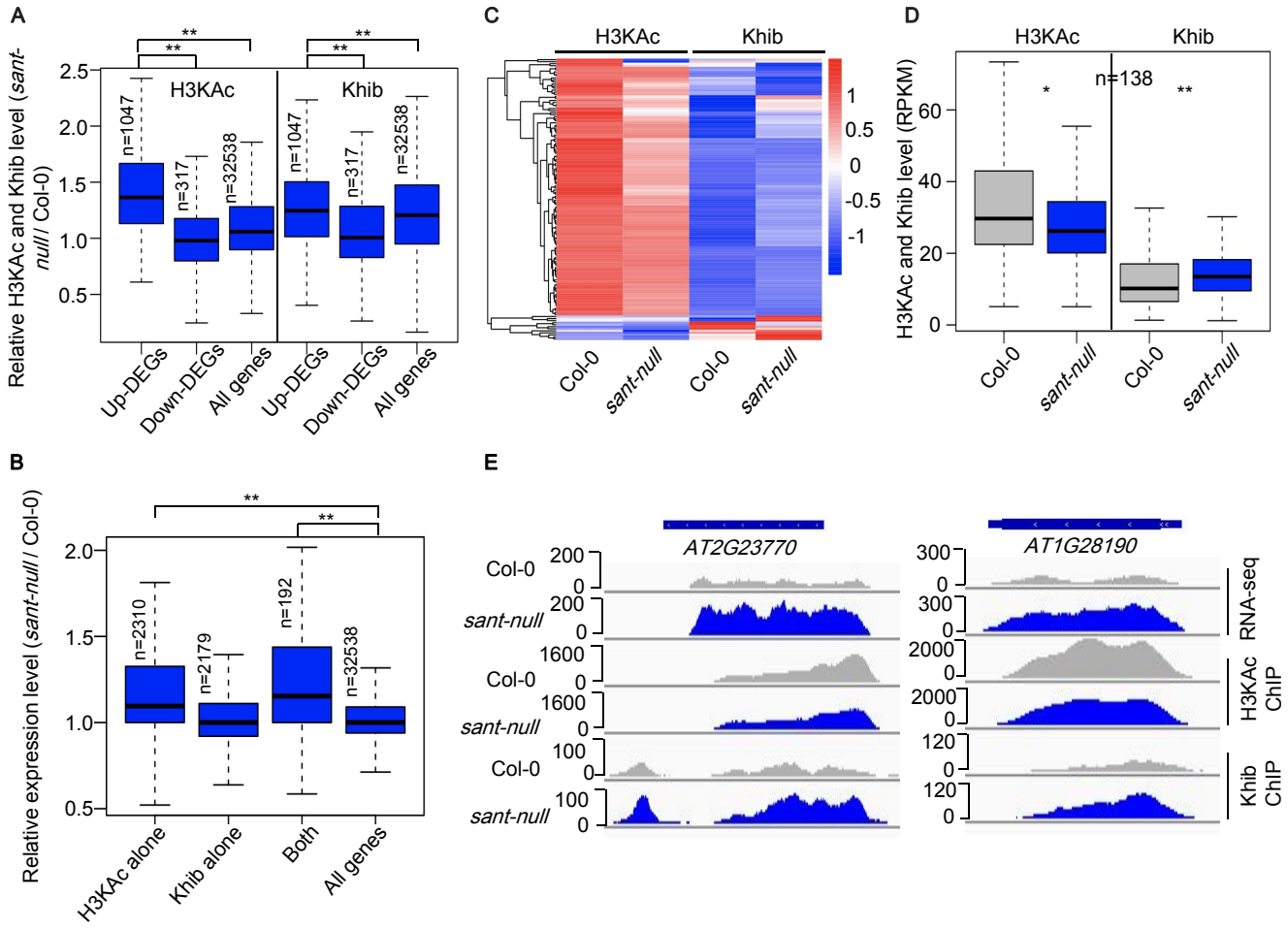
A
Relative H3KAc and Khib level (sant-null/ Col-0)
H3KAc
Khib
n=1047
n=317
n=32538
Up-DEGs
Down-DEGs
All genes
B
Relative expression level (sant-null/ Col-0)
n=2310
n=2179
n=192
n=32538
H3KAc alone
Khib alone
Both
All genes
C
H3KAc
Khib
Col-0
sant-null
D
H3KAc and Khib level (RPKM)
n=138
E
AT2G23770
AT1G28190
RNA-seq
H3KAc ChIP
Khib ChIP

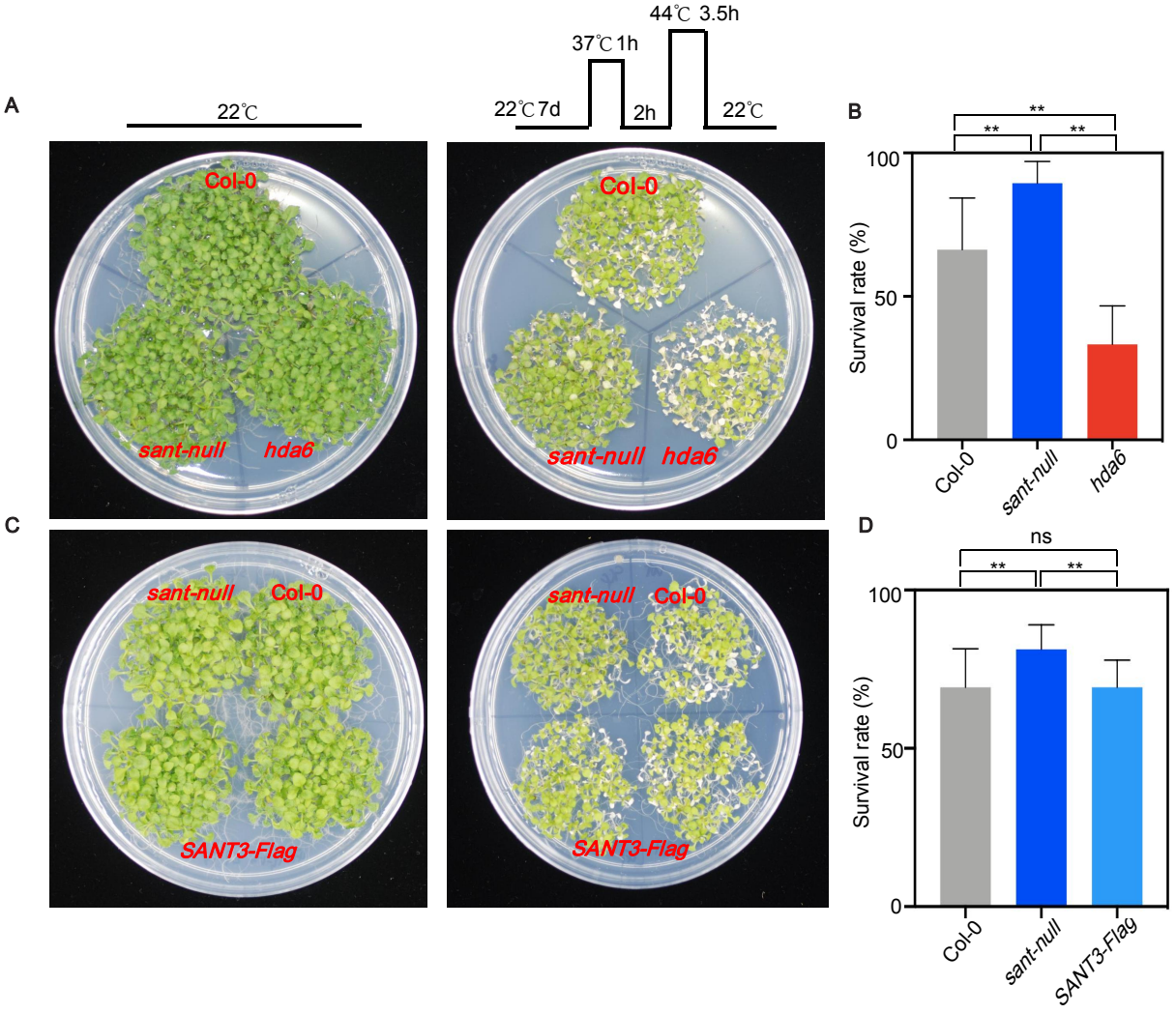
A
22℃
44℃ 3.5h
37℃ 1h
22℃ 7d
2h
22℃
Col-0
sant-null
hda6
Col-0
sant-null
hda6
B
**
**
**
Survival rate (%)
100
50
0
Col-0
sant-null
hda6
C
sant-null
Col-0
SANT3-Flag
sant-null
Col-0
SANT3-Flag
D
ns
**
**
Survival rate (%)
100
50
0
Col-0
sant-null
SANT3-Flag

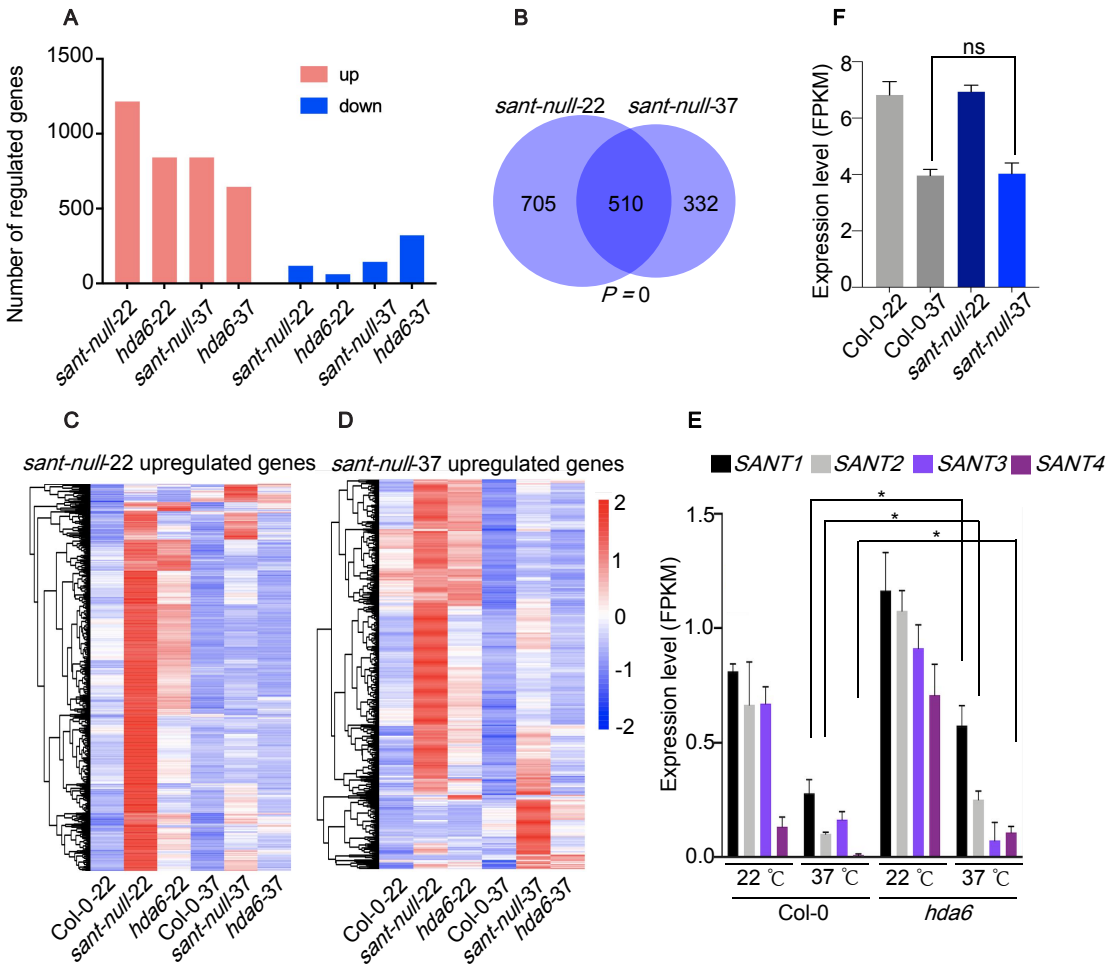
A
Number of regulated genes
1500
1000
500
0
up
down
sant-null-22
hda6-22
sant-null-37
hda6-37
sant-null-22
hda6-22
sant-null-37
hda6-37
B
sant-null-22
sant-null-37
705
510
332
P = 0
F
ns
Expression level (FPKM)
8
6
4
2
0
Col-0-22
Col-0-37
sant-null-22
sant-null-37
C
sant-null-22 upregulated genes
Col-0-22
sant-null-22
hda6-22
Col-0-37
sant-null-37
hda6-37
D
sant-null-37 upregulated genes
2
1
0
-1
-2
Col-0-22
sant-null-22
hda6-22
Col-0-37
sant-null-37
hda6-37
E
SANT1
SANT2
SANT3
SANT4
Expression level (FPKM)
1.5
1.0
0.5
0.0
*
*
*
22 ℃
37 ℃
22 ℃
37 ℃
Col-0
hda6

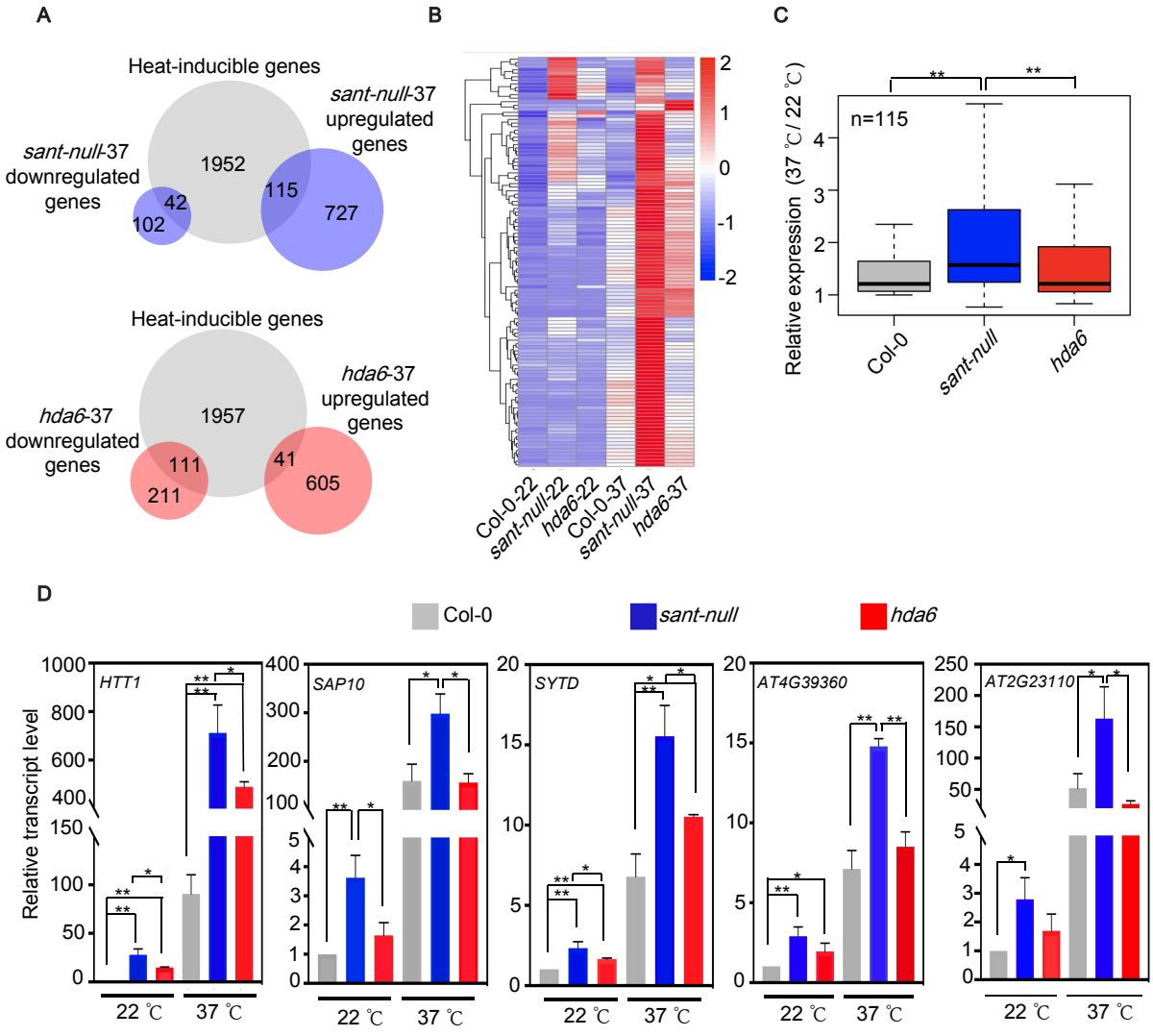
A
Heat-inducible genes
sant-null-37 upregulated genes
sant-null-37 downregulated genes
1952
115
42
102
727
Heat-inducible genes
hda6-37 upregulated genes
hda6-37 downregulated genes
1957
41
111
211
605
B
2
1
0
-1
-2
Col-0-22
sant-null-22
hda6-22
Col-0-37
sant-null-37
hda6-37
C
n=115
Relative expression (37 ℃/ 22 ℃)
Col-0
sant-null
hda6
D
Col-0
sant-null
hda6
Relative transcript level
HTT1
SAP10
SYTD
AT4G39360
AT2G23110
22 ℃
37 ℃

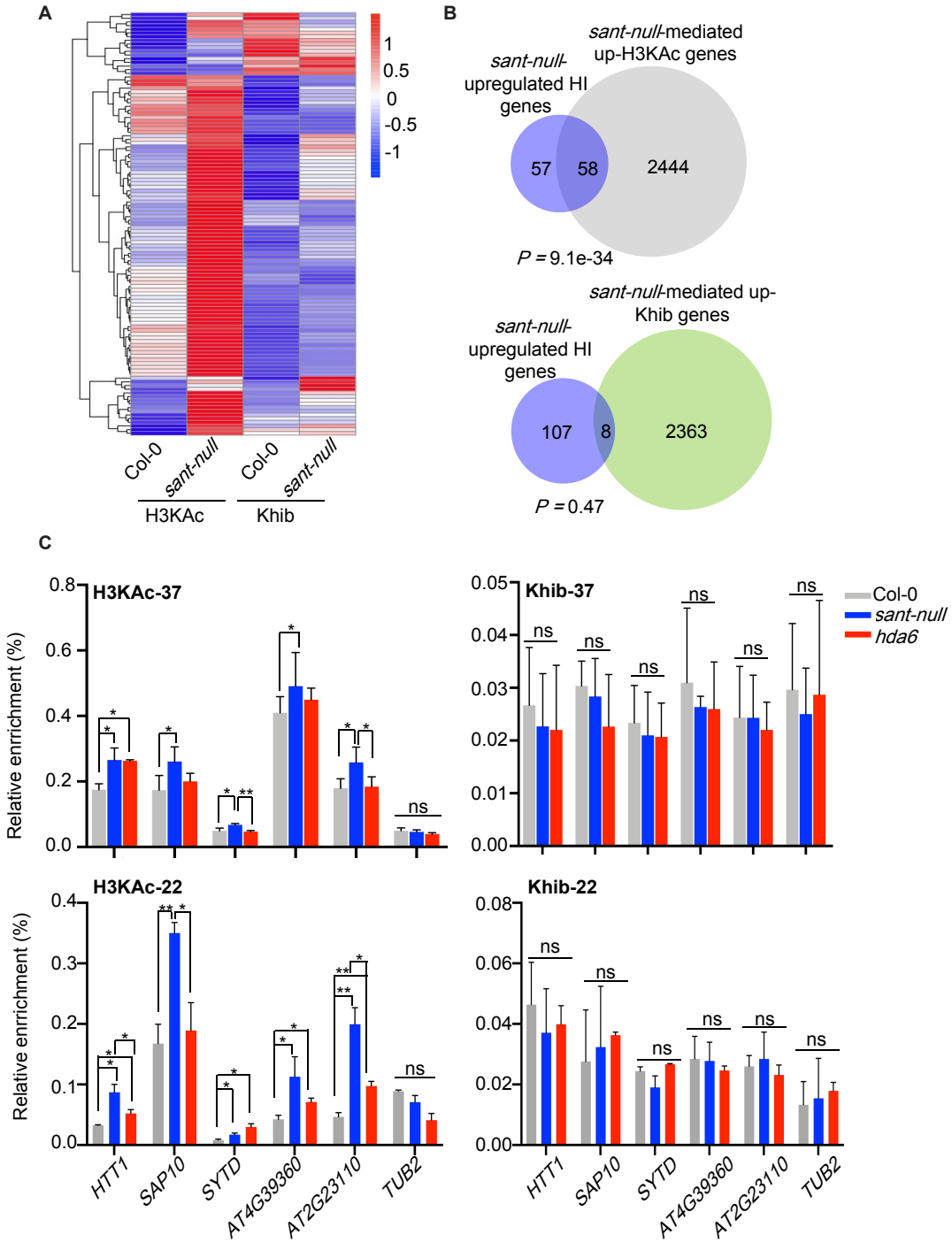
A
1
0.5
0
-0.5
-1
Col-0
sant-null
Col-0
sant-null
H3KAc
Khib
B
sant-null-mediated up-H3KAc genes
sant-null-upregulated HI genes
57
58
2444
P = 9.1e-34
sant-null-mediated up-Khib genes
sant-null-upregulated HI genes
107
8
2363
P = 0.47
C
H3KAc-37
Khib-37
Col-0
sant-null
hda6
Relative enrrichment (%)
H3KAc-22
Khib-22
HTT1
SAP10
SYTD
AT4G39360
AT2G23110
TUB2
ns

Parsed Citations

Allfrey, VG., Faulkner, R., and Mirsky, A. (1964). Acetylation and methylation of histones and their possible role in the regulation of RNA synthesis. Proceedings of the National Academy of Sciences, USA 51(5): 786-794.
Google Scholar: Author Only Title Only Author and Title

Bourgine, B., and Guihur, A. (2021). Heat shock signaling in land plants: from plasma membrane sensing to the transcription of small heat shock proteins. Frontiers in Plant Science 12: 710801.
Google Scholar: Author Only Title Only Author and Title

Chen, Y., Sprung, R., Tang, Y., Ball, H., Sangras, B., Kim, SC., Falck, JR., Peng, J., Gu, W., and Zhao, Y. (2007). Lysine propionylation and butyrylation are novel post-translational modifications in histones. Molecular & Cellular Proteomics 6 (5): 812–819.
Google Scholar: Author Only Title Only Author and Title

Dai, L., Peng, C., Montellier, E., Lu, Z., Chen, Y., Ishii, H., Debernardi, A., Buchou, T., Rousseaux, S., Jin, F., et al. (2014). Lysine 2-hydroxyisobutyrylation is a widely distributed active histone mark. Nature Chemical Biology 10 (5): 365-370.
Google Scholar: Author Only Title Only Author and Title

Duan, CG., Wang, X., Xie, S., Pan, L., Miki, D., Tang, K., Hsu, CC., Lei, M., Zhong, Y., Hou, YJ., et al. (2017). A pair of transposon-derived proteins function in a histone acetyltransferase complex for active DNA demethylation. Cell Research. 27(2): 226-240.
Google Scholar: Author Only Title Only Author and Title

Feng, C., Cai, X., Su, Y., L, L., Chen, S., and He, X. (2021). Arabidopsis RPD3-like histone deacetylases form multiple complexes involved in stress response. Journal of Genetics and Genomics 48 (5): 369-383.
Google Scholar: Author Only Title Only Author and Title

Friedrich, T., Oberkofler, V., Trindade, I., Altmann, S., Brzezinka, K., Lämke, J., Gorka, M., Kappel, C., Sokolowska, E., Skirycz, A., et al. (2021). Heteromeric HSFA2/HSFA3 complexes drive transcriptional memory after heat stress in Arabidopsis. Nat Communications 12 (1):3426.
Google Scholar: Author Only Title Only Author and Title

Garcia, BA., Shabanowitz, J., and Hunt, DF. (2007). Characterization of histones and their post-translational modifications by mass spectrometry. Current Opinion in Chemical Biology 11(1): 66-73.
Google Scholar: Author Only Title Only Author and Title

He, Y., and Li, Z. (2018). Epigenetic environmental memories in plants: establishment, maintenance, reprogramming. Trends in Genetics 34 (11): 856–866.
Google Scholar: Author Only Title Only Author and Title

Hu, Y., Lu, Y., Zhao, Y., and Zhou, DX. (2019). Histone acetylation dynamics integrates metabolic activity to regulate plant response to stress. Frontiers in Plant Science 10: 1236.
Google Scholar: Author Only Title Only Author and Title

Hu. Z., Song, N., Zheng, M., Liu, X., Liu, Z., Xing, J., Ma, J., Guo, W., Yao, Y., Peng, H., et al. (2015). Histone acetyltransferase GCN5 is essential for heat stress-responsive gene activation and thermotolerance in Arabidopsis. The Plant Journal 84(6): 1178–1191.
Google Scholar: Author Only Title Only Author and Title

Huang, H., Luo, Z., Qi, S., Huang, J., Xu, P., Wang, X., Gao, L., Li, F., Wang, J., Zhao, W., et al. (2018). Landscape of the regulatory elements for lysine 2-hydroxyisobutyrylation pathway. Cell Research 28(1): 111-125.
Google Scholar: Author Only Title Only Author and Title

Huang, J., Luo, Z., Ying, W., Cao, Q., Huang, H., Dong, J., Wu, Q., Zhao, Y., Qian, X., and Dai, J. (2017). 2-Hydroxyisobutyrylation on histone H4K8 is regulated by glucose homeostasis in Saccharomyces cerevisiae. Proceedings of the National Academy of Sciences, USA 114 (33): 8782-8787.
Google Scholar: Author Only Title Only Author and Title

Kapitonov, VV., and Jurka, J. (2004). Harbinger transposons and an ancient HARBI1 gene derived from a transposase. DNA and Cell Biology. 23(5): 311-324.
Google Scholar: Author Only Title Only Author and Title

Kebede, AF., Nieborak, A., Shahidian, LZ., Le, Gras S., Richter, F., Gómez, DA., Baltissen, MP., Meszaros, G., Magliarelli, HF., Taudt, A., et al. (2017). Histone propionylation is a mark of active chromatin. Nature Structural & Molecular Biology 24 (12): 1048-1056.
Google Scholar: Author Only Title Only Author and Title

Kim, YJ., Wang, R., Gao, L., Li, D., Xu, C., Mang, H., Jeon, J., Chen, X., Zhong, X., Kwak, JM., et al. (2016). Powerdress and HDA9 interact and promote histone H3 deacetylation at specific genomic sites in Arabidopsis. Proceedings of the National Academy of Sciences, USA 113(51):14858–14863.
Google Scholar: Author Only Title Only Author and Title

Langmead, B., and Salzberg, SL. (2012). Fast gapped-read alignment with Bowtie 2. Nature Methods 9 (4): 357-359.
Google Scholar: Author Only Title Only Author and Title

Li, S., Liu, J., Liu, Z., Li, X., Wu, F., and He, Y. (2014). HEAT-INDUCED TAS1 TARGET1 mediates thermotolerance via HEAT STRESS TRANSCRIPTION FACTOR A1a-directed pathways in Arabidopsis. The Plant Cell 26(4):1764-1780.
Google Scholar: Author Only Title Only Author and Title

Liang, SC., Hartwig, B., Perera, P., Mora-García, S., Leau, E.d., Thornton, H., Alves, F.d.L., Rappsilber, J., Yang, S., James, GV., et al. (2015). Kicking against the PRCs- A Domesticated Transposase Antagonises Silencing Mediated by Polycomb Group Proteins and Is an Accessory Component of Polycomb Repressive Complex 2. PLOS Genetics 11(12): e1005660.
Google Scholar: Author Only Title Only Author and Title

Lim, CJ., Park, J., Shen, M., Park, HJ., Cheong, MS., Park, KS., Baek, D., Bae, MJ., Ali, A., Jan, M., et al. (2020). The Histone-Modifying Complex PWR/HOS15/HD2C Epigenetically Regulates Cold Tolerance. Plant Physiology 184 (2):1097-1111.
Google Scholar: Author Only Title Only Author and Title

Lu, Y., Xu, Q., Liu, Y., Yu, Y., Cheng, ZY., Zhao, Y., and Zhou, DX. (2018). Dynamics and functional interplay of histone lysine butyrylation, crotonylation, and acetylation in rice under starvation and submergence. Genome Biology 19 (1): 144.
Google Scholar: Author Only Title Only Author and Title

Mayer, KS., Chen, X., Sanders, D., Chen, J., Jiang, J., Nguyen, P., Scalf, M., Smith, LM., and Zhong, X. (2019). HDA9-PWR-HOS15 is a core histone deacetylase complex regulating transcription and development. Plant Physiology 180 (1): 342–355.
Google Scholar: Author Only Title Only Author and Title

Niu, Y., Bai, J., Liu, X., Zhang, H., Bao, J., Zhao, W., Hou, Y., Deng, X., Yang, C., Guo, L., et al. (2022). HISTONE DEACETYLASE 9 transduces heat signal in plant cells. Proceedings of the National Academy of Sciences, USA 119(45) :e2206846119.
Google Scholar: Author Only Title Only Author and Title

Park, HJ., Baek, D., Cha, JY., Liao, X., Kang, SH., McClung, CR., Lee, SY., Yun, DJ., and Kim, WY. (2019). HOS15 interacts with the histone deacetylase HDA9 and the evening complex to epigenetically regulate the floral activator GI- GANTEA. The Plant Cell 31(1): 37–51.
Google Scholar: Author Only Title Only Author and Title

Patil, V., and Nandi, AK. (2022). POWERDRESS positively regulates systemic acquired resistance in Arabidopsis. Plant Cell Reports 41(12):2351-2362.
Google Scholar: Author Only Title Only Author and Title

Perrella, G., Baurle, I., and Zanten, M.v. (2022). Epigenetic regulation of thermomorphogenesis and heat stress tolerance. New Phytologist 234 (4): 1144–1160.
Google Scholar: Author Only Title Only Author and Title

Sabari, BR., Zhang, D., Allis, CD., and Zhao, Y. (2017). Metabolic regulation of gene expression through histone acylations. Nature Reviews Molecular Cell Biology 18 (2):90–101.
Google Scholar: Author Only Title Only Author and Title

Shahbazian, MD., and Grunstein, M. (2007). Functions of site-specific histone acetylation and deacetylation. Annual Review of Biochemistry 76: 75-100.
Google Scholar: Author Only Title Only Author and Title

Tarasov, A., Vilella, AJ., Cuppen, E., Nijman, IJ., and Prins, P. (2015). Sambamba: fast processing of NGS alignment formats. Bioinformatics 31(12): 2032-2034.
Google Scholar: Author Only Title Only Author and Title

Castellanos, R.U., Friedrich, T., Petrovic, N., Altmann, S., Brzezinka, K., Gorka, M., Graf, A., and Bäurle, I. (2020). FORGETTER2 protein phosphatase and phospholipase d modulate heat stress memory in Arabidopsis. The Plant Journal 104 (1), 7–17.
Google Scholar: Author Only Title Only Author and Title

Velanis, CN., Perera, P., Thomson, B., Leau, E.d., Liang, S.C., Hartwig, B., Förderer, A., Thornton, H., Arede, P., Chen, J., et al. (2020). The domesticated transposase ALP2 mediates formation of a novel Polycomb protein complex by direct interaction with MSI1, a core subunit of Polycomb Repressive Complex 2 (PRC2). PLOS Genetics 16(5): e1008681.
Google Scholar: Author Only Title Only Author and Title

Wang, S., Wang, M., Ichino, L., Boone, BA., Zhong, Z., Papareddy, RK., Lin, EK., Yun, J., Feng, S., and Jacobsen, SE. (2024). MBD2 couples DNA methylation to transposable element silencing during male gametogenesis. Nature Plants 10 (1):13-24.
Google Scholar: Author Only Title Only Author and Title

Wang, Y., Hu, Q., Wu, Z., Wang, H., Han, S., Jin, Y., Zhou, J., Zhang, Z., Jiang, J., Shen, Y., et al. (2017). HISTONE DEACETYLASE 6 represses pathogen defence responses in Arabidopsis thaliana. Plant, Cell & Environment 40 (12):2972–2986.
Google Scholar: Author Only Title Only Author and Title

Yamaguchi, N., Matsubara, S., Yoshimizu, K., Seki, M., Hamada, K., Kamitani, M., Kurita, Y., Nomura, Y., Nagashima, K., Inagaki, S., et al. (2021). H3K27me3 demethylases alter HSP22 and HSP17.6C expression in response to recurring heat in Arabidopsis. Nature Communications 12(1):3480.
Google Scholar: Author Only Title Only Author and Title

Yang, F., Sun, Y., Du, X., Chu, Z., Zhong, X., and Chen, X. (2023). Plant-specific histone deacetylases associate with ARGONAUTE4 to promote heterochromatin stabilization and plant heat tolerance. New Phytologist 238(1):252-269.
Google Scholar: Author Only Title Only Author and Title

Yang, L., Chen, X., Wang, Z., Sun, Q., Hong, A., Zhang, A., Zhong, X., and Hua, J. (2020). HOS15 and HDA9 negatively regulate immunity through histone deacetylation of intracellular immune receptor NLR genes in Arabidopsis. New Phytologist 226 (2): 507–522.
Google Scholar: Author Only Title Only Author and Title

Yruela, I., Moreno-Yruela, C., and Olsen, C.A. (2021). Zn2+-Dependent histone deacetylases in plants: structure and evolution. Trends in Plant Science 26 (7):741-757.
Google Scholar: Author Only Title Only Author and Title

Yu, G., Wang, LG., Han, Y., and He, QY. (2012). clusterProfiler: an R package for comparing biological themes among gene clusters. Omics 16(5):284-287.
Google Scholar: Author Only Title Only Author and Title

Yu, Z., Ni, J., Sheng, W., Wang, Z., and Wu, Y. (2017). Proteome-wide identification of lysine 2-hydroxyisobutyrylation reveals conserved and novel histone modifications in Physcomitrella patens. Scientific Reports 7(1):15553.
Google Scholar: Author Only Title Only Author and Title

Zhang, K., Sridhar, V.V., Zhu, J., Kapoor, A., and Zhu, JK. (2007). Distinctive core histone post-translational modification patterns in Arabidopsis thaliana. PLOS ONE 2(11): e1210.
Google Scholar: Author Only Title Only Author and Title

Zhang, N., Zhang, L., Li, L., Geng, J., Zhao, L., Ren, Y., Dong, Z., and Chen, F. (2022). Global Profiling of 2-hydroxyisobutyrylome in Common Wheat. Genomics, Proteomics & Bioinformatics 20(4):688-701.
Google Scholar: Author Only Title Only Author and Title

Zhang, X., Jiang, N., Feschotte, C., and Wessler, S.R. (2004). PIF- and Pong-like transposable elements: distribution, evolution and relationship with Tourist-like miniature inverted-repeat transposable elements. Genetics 166 (2): 971-986.
Google Scholar: Author Only Title Only Author and Title

Zhao, T., Zhan, Z., and Jiang, D. (2019). Histone modifications and their regulatory roles in plant development and environmental memory. Journal of Genetics and Genomics 46 (10): 467-476.
Google Scholar: Author Only Title Only Author and Title

Zheng, L., Li, C., Ma, X., Zhou, H., Liu, Y., Wang, P., Yang, H., Tamada, Y., Huang, J., Wang, C., et al. (2021). Functional interplay of histone lysine 2-hydroxyisobutyrylation and acetylation in Arabidopsis under dark-induced starvation. Nucleic Acids Research 49(13) : 7347-7360.
Google Scholar: Author Only Title Only Author and Title

Zhou, X., He, J., Velanis, C.N., Zhu, Y., He, Y., Tang, K., Zhu, M., Graser, L., Leau, E.d., Wang, X., et al. (2021). A domesticated Harbinger transposase forms a complex with HDA6 and promotes histone H3 deacetylation at genes but not TEs in Arabidopsis. Journal of Integrative Plant Biology 63(8): 1462–1474.
Google Scholar: Author Only Title Only Author and Title